Stem Cell Reports
Article

OPEN ACCESS

The aPKC-CBP Pathway Regulates Adult Hippocampal Neurogenesis in an Age-Dependent Manner

Ayden Gouveia,[1,2,10] Karolynn Hsu,[1,10] Yosuke Niibori,[5] Matthew Seegobin,[1] Gonzalo I. Cancino,[5] Ling He,[8] Fredric E. Wondisford,[9] Steffany Bennett,[3,4] Diane Lagace,[2,3] Paul W. Frankland,[5,6,7] and Jing Wang[1,2,3,*]

[1]Regenerative Medicine Program, Ottawa Hospital Research Institute, Ottawa, ON K1H 8L6, Canada
[2]Department of Cellular and Molecular Medicine
[3]Brain and Mind Research Institute
[4]Department of Biochemistry, Microbiology and Immunology
University of Ottawa, Ottawa, ON K1H 8M5, Canada
[5]Neurosciences and Mental Health, Hospital for Sick Children, Toronto, ON M5G 1X8, Canada
[6]Department of Psychology
[7]Department of Physiology
University of Toronto, Toronto, ON M5G 1X5, Canada
[8]Division of Metabolism, Department of Pediatrics, Johns Hopkins Medical School, Baltimore, MD 21287, USA
[9]Department of Medicine and Pediatrics, Rutgers-Robert Wood Johnson Medical School, New Brunswick, NJ 08901, USA
[10]Co-first author
*Correspondence: jiwang@ohri.ca
http://dx.doi.org/10.1016/j.stemcr.2016.08.007

SUMMARY

While epigenetic modifications have emerged as attractive substrates to integrate environmental changes into the determination of cell identity and function, specific signals that directly activate these epigenetic modifications remain unknown. Here, we examine the role of atypical protein kinase C (aPKC)-mediated Ser436 phosphorylation of CBP, a histone acetyltransferase, in adult hippocampal neurogenesis and memory. Using a knockin mouse strain (*Cbp*S436A) in which the aPKC-CBP pathway is deficient, we observe impaired hippocampal neuronal differentiation, maturation, and memory and diminished binding of CBP to CREB in 6-month-old C*bp*S436A mice, but not at 3 months of age. Importantly, elevation of CREB activity rescues these deficits, and CREB activity is reduced whereas aPKC activity is increased in the murine hippocampus as they age from 3 to 6 months regardless of genotype. Thus, the aPKC-CBP pathway is a homeostatic compensatory mechanism that modulates hippocampal neurogenesis and memory in an age-dependent manner in response to reduced CREB activity.

INTRODUCTION

Newborn neurons are continuously generated throughout life in several areas of the mammalian brain, including the subgranular zone (SGZ) of the hippocampal dentate gyrus (Imayoshi et al., 2008; Palmer et al., 1997; Zhao et al., 2008). Adult hippocampal neurogenesis is essential for neuronal addition and hippocampal growth, potentially contributing to new memory formation during adulthood (Deng et al., 2010; Dupret et al., 2007; Imayoshi et al., 2008; Sahay et al., 2011; Saxe et al., 2006). Adult neural precursor cells (NPCs) in the SGZ predominantly give rise to transit-amplifying cells and neuroblasts, which ultimately generate granule neurons in the hippocampal dentate gyrus (Ming and Song, 2011; Toni et al., 2008; Wang et al., 2012; Zhao et al., 2008). An early and dramatic decline in hippocampal neurogenesis that occurs in mice during early adulthood (3–6 months) is associated with a reduction in neural progenitor proliferation and newborn neuron survival (Kuipers et al., 2015). In contrast, the rate of neuronal differentiation is constant during early adulthood and remains sustained even in older (1–1.5 years old) mice (Kuipers et al., 2015). Disruption of this ongoing neurogenesis has been proposed to play a role in progressive neurodegenerative disorders such as Alzheimer's disease (Mu and Gage, 2011; Winner et al., 2011; Zhao et al., 2008). Therefore, understanding the underlying molecular mechanisms that sustain the age-dependent hippocampal neurogenesis will provide a fundamental basis to elucidate the pathogenesis and therapeutic targets of Alzheimer's disease.

We previously showed that an atypical protein kinase C-CREB binding protein (aPKC-CBP) pathway is important for the differentiation of embryonic NPCs into all three neural cell lineages: neurons, astrocytes, and oligodendrocytes (Wang et al., 2010). Specifically, we demonstrated that activation of aPKC leads to Ser436 phosphorylation in CBP, a histone acetyltransferase, and that this phosphorylation causes transcription of genes that are associated with the three cell lineages. Moreover, we demonstrated that metformin, an AMP kinase (AMPK) activator, could activate the aPKC-CBP pathway to promote neurogenesis and enhance spatial memory formation in adult mice (Wang et al., 2012; Fatt et al., 2015). Interestingly, another recent study demonstrated that CBP is required for enriched environment-induced adult

hippocampal neurogenesis and learning and memory (Lopez-Atalaya et al., 2011). Together, these findings suggest that CBP-mediated epigenetic regulation plays a central role in integrating environmental/microenvironmental changes to the determination of NPC differentiation in the developing and adult brain.

The specificity of CBP actions is determined by its transcription factor binding partners. One of the binding partners is CREB (cyclic AMP response element binding protein), which is known to play a central role in regulating hippocampal plasticity, neurogenesis, and memory formation (Merz et al., 2011; Mizuno et al., 2002; Nakagawa et al., 2002a; Silva et al., 1998). When CREB is phosphorylated at Ser133, it recruits CBP and positively regulates CREB-mediated gene transcription (Parker et al., 1996; Shih et al., 1996). Intriguingly, the phosphorylated CREB at Ser133 (pS133-CREB) is stably expressed in doublecortin (DCX)-positive neuroblasts/newborn neurons in the hippocampal SGZ, suggesting its central role in neuronal differentiation and/or maturation (Merz et al., 2011). Moreover, previous work in liver cells has shown that aPKC-dependent Ser436 phosphorylation of CBP can regulate its association with CREB (He et al., 2009). These findings led us to test the hypothesis that activation of the aPKC-CBP pathway may modulate hippocampal neurogenesis and memory formation by regulating the association of CBP with CREB in the hippocampus.

Our findings show that the aPKC-CBP pathway is required for hippocampal neuronal differentiation and maturation and hippocampal-dependent memory in mature adult (6 months old) mice, but not in young adult (3 months old) mice. Mechanistically, we found that the aPKC-CBP pathway is highly upregulated and is necessary to maintain the association of CBP with CREB in the hippocampus of mature mice when CREB activity (pS133-CREB) is reduced. More importantly, elevation of CREB activity (pS133-CREB) by a phosphodiesterase 4 (PDE4) inhibitor, rolipram, in the hippocampus can rescue the neuronal differentiation and maturation deficits in mature mice. This rescue is also accompanied by restoring impaired pre-exposure fear memory and the diminished binding of CBP to CREB in *Cbp*S436A mice. Together, these data argue that the aPKC-CBP pathway has a compensatory homeostatic role in modulating hippocampal neurogenesis and hippocampal-dependent memory during early adulthood (3–6 months).

RESULTS

The aPKC-CBP Pathway Regulates Adult Neurogenesis

To ask whether the aPKC-mediated CBP S436 phosphorylation is important for adult hippocampal neurogenesis, we took advantage of a phosphor-mutant *Cbp*S436A knockin (*Cbp*S436A-KI) mouse strain in which the aPKC-CBP pathway is deficient due to the exchange of the serine (S) 436 residue for an alanine (A) residue in CBP. *Cbp*S436A-KI mice survive into adulthood, and do not exhibit any apparent changes in brain structure (data not shown). To assess adult hippocampal neurogenesis, we injected 3- and 6-month-old mice with bromodeoxyuridine (BrdU) (100 mg/kg, intraperitoneally) daily for 3 consecutive days, and euthanized the mice 12 days after the first BrdU injection. Hippocampi were analyzed by immunostaining for BrdU and the mature neuron marker NEUN. Quantification throughout the extent of the hippocampal dentate gyrus demonstrated a significant decrease in the total number of BrdU/NEUN-positive neurons in *Cbp*S436A-KI mice at both ages (Figures 1A and 1B).

To explore cellular mechanisms underlying the reduction in neurogenesis in the *Cbp*S436A-KI mice, we first investigated whether the number of proliferating NPCs was decreased using the proliferation marker, Ki-67. This analysis demonstrated that the number of Ki-67-positive proliferating NPCs in the SGZ was unchanged in *Cbp*S436A-KI mice at both 3 and 6 months of age (Figures 1C and 1D). We further immunostained sections for an apoptotic marker, cleaved caspase-3 (CC3), and a marker for neuroblasts/newborn neurons, doublecortin (DCX) (Figures 1E and 1F). We observed that ~80% of CC3-positive cells are DCX-positive neuroblasts/newborn neurons. Although the basal level of CC3-positive dying cells was low in wild-type (WT) mice (total 30–50 cells throughout the extent of hippocampus) at both ages, the number of DCX/CC3-positive cells was significantly increased in *Cbp*S436A-KI mice at the age of 3 months, but not 6 months (Figures 1E and 1F). These results suggest that young adult *Cbp*S436A-KI mice have a reduction in survival of newborn neurons, in the absence of changes in proliferation.

To further confirm that newborn cell survival was decreased in 3-month-old *Cbp*S436A-KI mice, we performed BrdU in vivo chasing experiments by quantifying the total number of surviving BrdU-positive cells at 1, 12, and 30 days following BrdU injections. Relative to their WT littermates, *Cbp*S436A-KI mice had no change in the total number of 1-day-old BrdU cells (Figures 1G and 1H), in agreement with no change in the proliferating Ki-67-positive cells (Figures 1C and 1D). In addition, consistent with less newborn cell survival (Figures 1E and 1F), there was a significant decrease in the total number of 12- and 30-day-old BrdU-positive cells in 3-month-old *Cbp*S436A-KI mice (Figures 1G and 1H). Further quantification of the number of BrdU/NEUN-positive neurons 30 days after BrdU labeling showed a sustained reduction in hippocampal neurogenesis in both 3- and 6-month-old *Cbp*S436A-KI mice (Figures 1I and 1J). We then assessed whether the

reduction in hippocampal neurogenesis was associated with a general decrease of adult neurogenesis by analyzing the same mice for olfactory bulb neurogenesis. The total number of adult-born BrdU/NEUN-positive neurons in the olfactory bulb was proportionately decreased in the 3-month-old *Cbp*S436A-KI mice (Figures S1A and S1B). Together, these findings suggest that a reduction of neurogenesis in young adult *Cbp*S436A-KI mice (3 months) is at least partly due to an increase in the death of neuroblasts/newborn neurons.

The aPKC-CBP Pathway Regulates Adult Hippocampal Neuronal Differentiation and Maturation in an Age-Dependent Manner

Since the aPKC-CBP pathway has been identified as a pro-differentiation pathway during embryonic brain development (Tsui et al., 2014; Wang et al., 2010), we determined whether the aPKC-CBP pathway also regulates hippocampal neuronal differentiation, thus contributing to the reduction in hippocampal neurogenesis in the young (3-month) and older (6-month) mice (Figures 1A and 1B). Using the 12-day BrdU chasing paradigm previously described, *Cbp*S436A-KI had a significant reduction in the proportion of newborn mature neurons to the total BrdU-labeled cells (% NEUN/BrdU$^+$ over BrdU$^+$) at the age of 6 months, but no change at 3 months (Figures 2A and 2B). The fact that the total number of BrdU-positive cells was unaltered in 6-month-old *Cbp*S436A-KI mice (Figure S2A) argues that the decreased rate of hippocampal neurogenesis (Figures 2A and 2B) likely contributes to the reduced hippocampal neurogenesis at the age of 6 months in *Cbp*S436A-KI mice (Figures 1A and 1B). Next, we stained sections from the same experiments with a neural precursor marker, SOX2, and BrdU. The proportion of SOX2$^+$ NPCs over total BrdU-labeled cells (% SOX2/BrdU$^+$ over BrdU$^+$) was significantly increased in *Cbp*S436A-KI mice at the age of 6 months but not 3 months (Figures 2C and 2D), corresponding to the decreased proportion of newborn neurons in *Cbp*S436A-KI mice at 6 months. We further assessed other types of NPCs, including GFAP$^+$ type 1 NPCs and TBR2$^+$ type 2/3 NPCs in 6-month-old *Cbp*S436A-KI mice. Under our experimental conditions, we observed a small population of BrdU/GFAP co-labeled cells located in the SGZ and did not detect BrdU/GFAP co-labeled hilar astrocytes. Quantitative analysis showed that the population of BrdU/GFAP/SOX2$^+$ type 1 NPCs was not changed in *Cbp*S436A-KI mice (Figures S2B and S2C). However, the proportion of TBR2$^+$ NPCs over total BrdU-labeled cells (% TBR2/BrdU$^+$ over BrdU$^+$) was significantly increased in *Cbp*S436A-KI mice at 6 months (Figures 2E and 2F). Further quantification from triple-stained sections for TBR2, SOX2, and BrdU showed that the proportion of both SOX2$^+$/TBR2$^+$ type 2a and SOX2$^-$/TBR2$^+$ type 2b/3 NPCs was elevated in 6-month-old *Cbp*S436A-KI mice (Figures 2E and 2F). These results revealed that lack of Ser436 phosphorylation in CBP leads to the impaired development of hippocampal NPCs at the age of 6 months by arresting them at the stage of TBR2- and or/SOX2-positive NPCs. Together, these data suggest that the aPKC-CBP pathway is required to maintain the sustained neuronal differentiation of hippocampal NPCs in mature adults (6 months).

We further assessed the population of DCX-positive neuroblasts/newborn neurons in *Cbp*S436A-KI mice. The total number of DCX-positive cells was not significantly different between WT and *Cbp*S436A-KI mice (Figures S2D and S2E) at either 3 or 6 months of age. We then examined BrdU-labeled DCX-positive cells at both ages. The proportion of BrdU-positive cells that express DCX (% DCX/BrdU$^+$ over BrdU$^+$) was not changed in *Cbp*S436A-KI mice at both 3 and 6 months (Figures 2G and 2H). In contrast, the total number of co-labeled BrdU/DCX-positive cells was decreased in 3-month-old *Cbp*S436A-KI (Figure S2F), as expected due to the reduced total number of BrdU-positive cells (Figures 1G, 1H, and S2A).

The reduced rate of neuronal differentiation combined with the unaltered number and proportion of DCX-positive cells at the age of 6 months in the *Cbp*S436A-KI mice led us to hypothesize that these mice may have an impaired neuronal maturation process, manifested by the reduced acquisition of a mature neuron phenotype in DCX-positive neuroblasts/newborn neurons. We tested this hypothesis by performing triple staining with BrdU, NEUN, and DCX in 3- and 6-month-old brain sections. As we expected, the proportion of mature neurons (NEUN$^+$) in the BrdU/DCX-positive cells (% NEUN/BrdU/DCX$^+$ over BrdU/DCX$^+$ cells) was significantly decreased in 6-month-old *Cbp*S436A-KI mice (Figures 3A and 3B), indicating the reduced acquisition rate of mature neuron phenotype (NEUN$^+$) in the total newborn neurons. Consistent with this, the proportion of maturing neurons (% NEUN$^+$/DCX$^+$ over BrdU$^+$ cells) (Figure 3C) as well as mature neurons that had exited the immature stage (% NEUN$^+$/DCX$^-$ over BrdU$^+$ cells) (Figure 3D) was significantly reduced. In contrast, the percentage of BrdU-labeled DCX-positive, NEUN-negative neuroblasts/immature neurons (% DCX$^+$/NEUN$^-$ over BrdU$^+$ cells) was increased in 6 month-old *Cbp*S436A-KI mice (Figure 3E). There was also a significant increase in the percentage of BrdU-positive cells that were both NEUN and DCX negative (% NEUN$^-$/DCX$^-$ over BrdU$^+$ cells), representing the NPC population (Figure 3F). Thus, all of these data argue that the aPKC-CBP pathway is required for both neuronal differentiation and maturation in mature adult hippocampi (6 months) (Figure 3G).

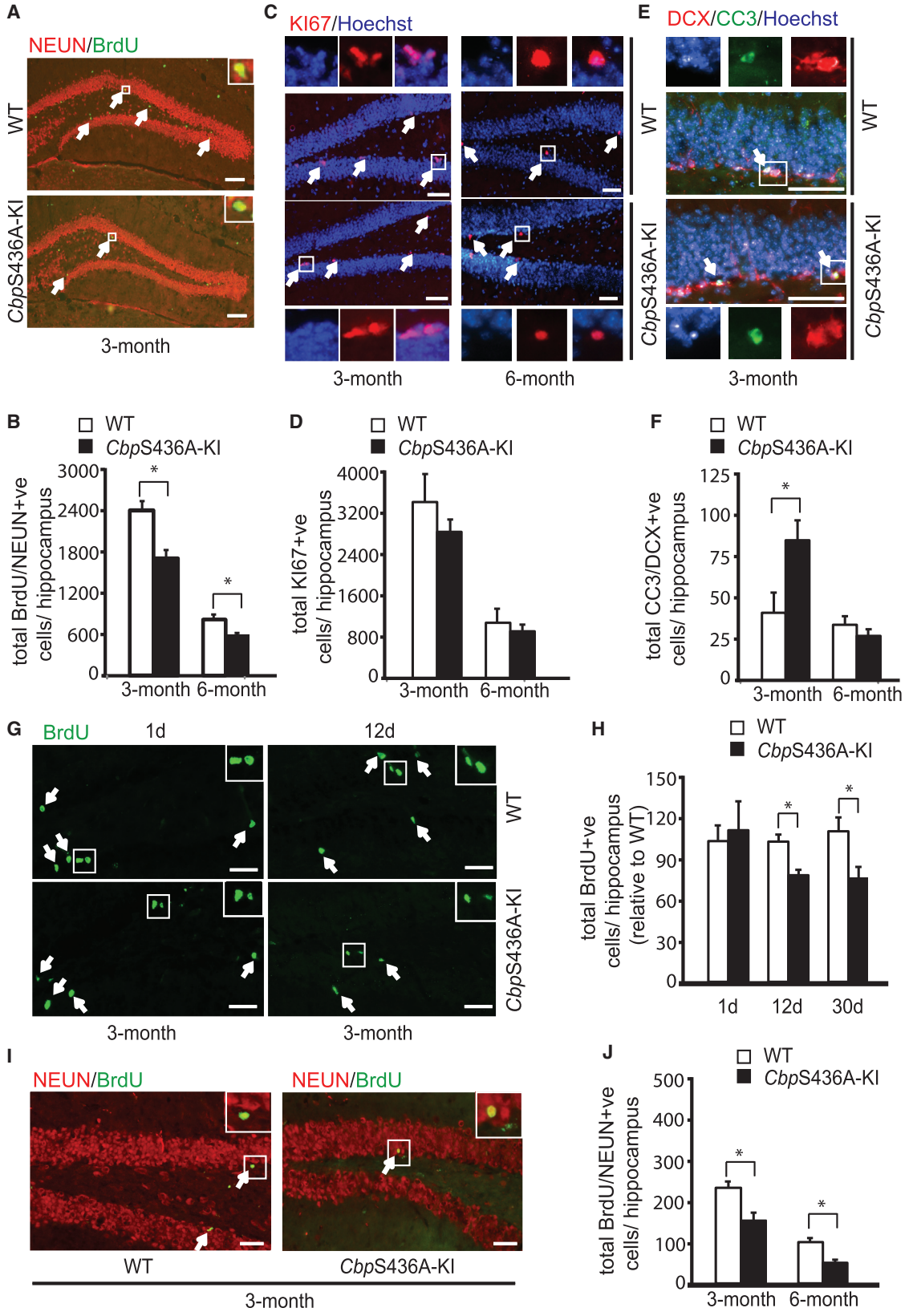

(legend on next page)

The aPKC-CBP Pathway Regulates Hippocampal-Dependent Fear Memory and Spatial Memory in Mature Adult Mice

Adult hippocampal neurogenesis plays a key role in hippocampal-dependent fear memory and spatial memory (Kee et al., 2007; Imayoshi et al., 2008; Saxe et al., 2006). Here we first used a context pre-exposure task, a version of contextual fear memory that is critically dependent on the hippocampus (Matus-Amat et al., 2004; Rudy et al., 2004), and is sensitive to detect deficits in adult neurogenesis (Cancino et al., 2013). In this task, the mice were first exposed to the context 24 hr before the foot shock to temporally separate the context acquisition phase from the association of the context with the shock (Figure 4A), unlike traditional context fear-conditioning experiments where the shock is introduced immediately after context exposure. Only animals that were pre-exposed to the context show high levels of freezing when subsequently tested (Fanselow, 2000). Consistent with an age-dependent reduction in hippocampal neuronal differentiation and maturation, the *Cbp*S436A-KI mice showed low freezing at 6 months but not at 3 months of age when compared with their respective WT littermates (Figures 4A and S3A).

We then used a hidden-platform version of the Morris water maze (MWM) task to measure spatial learning and memory in 6-month-old *Cbp*S436A-KI mice and their WT littermates. We showed that both WT and *Cbp*S436A-KI mice had a comparable learning curve over 7 days despite higher overall escape latency in *Cbp*S436A-KI mice (Figure 4B). We also analyzed the search strategies that the mice used through a visual algorithm analysis (Granger et al., 2016) to assess when the mice switched from a systematic to a spatial search strategy. We found that *Cbp*S436A-KI mice switched from systematic to spatial search strategies by training day 6, which was delayed compared with their WT littermates that switched by training day 4 (Figures 4C and 4D). Following the 7-day training session, probe tests were assessed at day 8 and day 19 by removing the platform from the swimming pool. At day 8, 24 hr after the last training, we observed that both *Cbp*S436A-KI and their WT littermates spent significantly more time in the target quadrant than in other three quadrants (Figure 4E), indicating normal short-term memory in *Cbp*S436A-KI mice. During the late probe test at day 19 (12 days after training), WT mice still spent significantly more time in the target quadrant relative to the other three quadrants while *Cbp*S436A-KI mice did not show a specific preference for the target quadrant (Figure 4F), suggesting impaired long-term spatial memory in *Cbp*S436A-KI mice. Finally, there was no difference in thigmotaxic swim patterns manifesting anxiety behaviors between WT and *Cbp*S436A-KI mice, implying that anxiety was not accountable for the impaired spatial learning and memory (Figures S3B–S3D). In addition, both WT and

Figure 1. Adult Mice Lacking CBPS436 Phosphorylation Show a Reduction in Adult Neurogenesis

(A) Fluorescence images of hippocampal sections from 3-month-old *Cbp*S436A (*Cbp*S436A-KI) and their wild-type littermates (WT), euthanized 12 days after BrdU injections and stained for BrdU (green) and NEUN (red). The insets show the boxed areas at higher magnification. Arrows represent double-labeled BrdU/NEUN-positive neurons. Scale bar, 100 μm.

(B) Quantitative analysis of the total number of BrdU/NEUN-positive newborn neurons in the hippocampi from 3- to 6-month-old WT and *Cbp*S436A-KI mice. *$p < 0.05$ ($n = 4–5$ animals for each group).

(C) Fluorescence images of hippocampal sections from 3- to 6-month-old WT and *Cbp*S436A-KI mice, immunostained for Ki-67 (KI67; red) and counterstained with Hoechst 33342 (blue). The boxed areas are shown at higher magnification in the top and bottom panels. Arrows denote Ki-67-positive proliferating cells. Scale bars, 50 μm.

(D) Quantitative analysis of the total number of Ki-67-positive proliferating cells in the hippocampi from 3- to 6-month-old *Cbp*S436A-KI and their WT littermates ($n = 4$ animals for each group).

(E) Fluorescence images of hippocampal sections from 3-month-old WT and *Cbp*S436A-KI mice, stained for cleaved caspase 3 (CC3) (green) and DCX (red). The boxed areas are shown at higher magnification in the top and bottom panels. Arrows denote double-labeled CC3/DCX-positive cells. Scale bars, 50 μm.

(F) Quantitative analysis of the total number of CC3/DCX-positive cells in the hippocampi from 3- to 6-month-old *Cbp*S436A-KI and their WT littermates. *$p < 0.05$ ($n = 4$ animals for each group).

(G) Fluorescence images of hippocampal sections from 3-month-old WT and *Cbp*S436A-KI mice 1 day and 12 days after BrdU injections, stained for BrdU (green). The insets show the boxed areas at higher magnification. Arrows denote BrdU-positive cells. Scale bars, 25 μm.

(H) Quantitative analysis of the total number of BrdU-positive cells in the hippocampi from 3-month-old WT and *Cbp*S436A-KI mice 1 day, 12 days, and 30 days following BrdU injections. *$p < 0.05$ ($n = 3–5$ animals for each group).

(I) Fluorescence images of hippocampal sections from 3-month-old WT and *Cbp*S436A-KI mice, euthanized 30 days after BrdU injections, and stained for BrdU (green) and NEUN (red). The insets show the boxed areas at higher magnification. Arrows represent double-labeled BrdU/NEUN-positive neurons. Scale bars, 25 μm.

(J) Quantitative analysis of the total number of BrdU/NEUN-positive neurons in the hippocampi from 3- to 6-month-old WT and *Cbp*S436A-KI mice. *$p < 0.05$ ($n = 4–5$ animals for each group).

Error bars represent SEM. See also Figure S1.

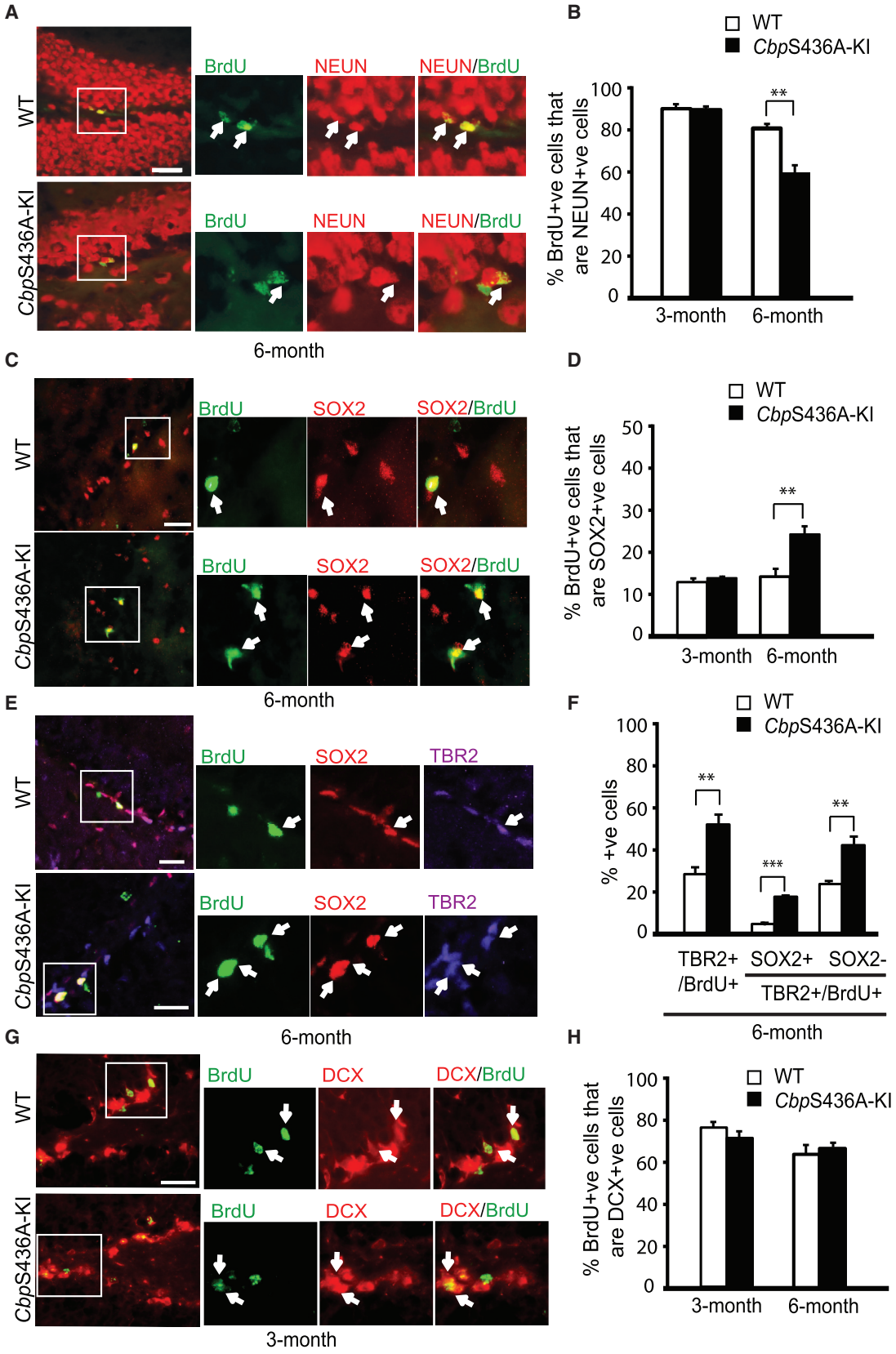

(legend on next page)

*Cbp*S436A-KI mice showed normal mean velocity, distance traveled, and anxiety behaviors in the open field (Figures 4G, S3E, and S3F), making it unlikely that the spatial and contextual memory deficits are attributable to non-specific impairments in motor function or increases in anxiety. Together, these data suggest that the aPKC-CBP pathway is essential for the regulation of age-dependent hippocampal-dependent fear and spatial learning and memory.

The aPKC-CBP Pathway Regulates CBP Binding to CREB in an Age-Dependent Manner

CREB is a major regulator of adult hippocampal neurogenesis and hippocampal-dependent learning and memory (Merz et al., 2011; Mizuno et al., 2002; Silva et al., 1998). Here, we assessed the ability of CBP to bind to CREB in *Cbp*S436A-KI hippocampal tissues at both 3 and 6 months of age using a co-immunoprecipitation assay. A reduction of the association of CBP with CREB was observed in hippocampal extracts obtained from mature (6 months old) but not young (3 months old) *Cbp*S436A-KI mice (Figures 5A and 5B). We further assessed the phosphorylation status of CREB at S133 (pS133-CREB), which is known to be a rate-limiting step in the association of CREB with CBP, and the level of aPKC activity, manifested by phosphorylation of threonine (pT)410/403-aPKC. Western blot analysis showed that WT mice exhibited a significant reduction in pS133-CREB and a robust enhancement in pT410/403-aPKC in hippocampal extracts as mice aged from 3 to 6 months (Figures 5C and 5D). *Cbp*S436A-KI mice similarly had a reduction in pS133-CREB and enhancement in pT410/403-aPKC with aging, although the basal level of pS133-CREB is slightly higher at 3 months in *Cbp*S436A-KI than in WT mice (Figures 5C and 5D). Furthermore, we confirmed that the protein levels of total CREB and aPKC remained unchanged between 3 and 6 months of age in the WT and *Cbp*S436A-KI mice (Figure 5E). These results suggest a model in which the aPKC-CBP pathway plays a compensatory role to maintain the interaction between CBP and CREB in mature adult hippocampi (6 months) in response to a reduced level of pS133-CREB. When the aPKC-CBP pathway is deficient in *Cbp*S436A-KI mice, the association of CBP with CREB is diminished in mature adult hippocampi (6 months) due to lack of phosphorylation in both CREB-S133 and CBP-S436, although the upstream kinase aPKC activity is highly upregulated.

Elevation of CREB Phosphorylation Rescues Neurogenesis Deficits, Impairs Fear Memory, and Restores CBP Binding to CREB in Mature Adult *Cbp*S436A Mice

To further test the model, we asked whether the elevation of pS133-CREB would rescue the cellular, molecular, and behavioral deficits observed in mature adult *Cbp*S436A-KI mice (6 months old). To do this we injected rolipram (1.25 mg/kg/day, intraperitoneally), a specific PDE4 inhibitor, for 14 days in vivo. As expected, we found that rolipram treatment increased pS133-CREB expressions as detected by western blot analysis in 6-month-old WT and *Cbp*S436A-KI hippocampal tissues (Figures 6A and 6B). Notably, immunohistochemistry analysis further showed that pS133-CREB is highly expressed in the hippocampal SGZ and most pS133-CREB positive cells in the hippocampi are DCX-positive cells (Figure S4A), supporting the transcription factor's role in the acquisition and maturation of DCX-positive neuroblasts/newborn neurons. Quantification of pS133-CREB-positive cells in the dentate gyrus indicated that rolipram treatment significantly increased the number of pS133-CREB positive cells in the 6-month-old hippocampal SGZ (Figure S4B), further validating the western blot analysis (Figures 6A and 6B).

To assess neurogenesis, we administered rolipram injections (1.25 mg/kg/day, intraperitoneally) for 14 days; BrdU co-injections were given at days 3–5 (100 mg/kg/day, intraperitoneally), and mice were euthanized at the end of 14 days to follow the same 12-day BrdU chasing

Figure 2. Mature Adult Mice Lacking CBPS436 Phosphorylation Show Reduced Hippocampal Neuronal Differentiation

Adult mice (3 and 6 months old) received BrdU (100 mg/kg) injections for 3 consecutive days, and were euthanized for immunostaining analysis 12 days after the first BrdU injection.

(A, C, E, and G) Fluorescence images of hippocampal sections from 6-month-old (A,C,E) and 3-month-old (G) WT and *Cbp*S436A-KI mice, stained for: (A) BrdU (green) and NEUN (red); (C) BrdU (green) and SOX2 (red); (E) BrdU (green), TBR2 (purple), and SOX2 (red); and (G) BrdU (green) and DCX (red). Arrows denote double-labeled cells. The boxed areas are shown at higher magnification on the right. Scale bars, 25 μm.

(B) Quantitative analysis of the percentage of BrdU-positive cells that express a mature neuron marker, NEUN, in the hippocampi from 3- to 6-month-old WT and *Cbp*S436A-KI mice. $^{**}p < 0.01$ (n = 4 animals for each group).

(D) Quantitative analysis of the percentage of BrdU-positive cells that were positive for SOX2 in the hippocampi from WT and *Cbp*S436A-KI mice at the ages of 3 and 6 months. $^{**}p < 0.01$ (n = 4 animals for each group).

(F) Quantitative analysis of the percentage of BrdU-positive cells that were positive for TBR2 and SOX2 in the hippocampi from WT and *Cbp*S436A-KI mice at 6 months. $^{**}p < 0.01$, $^{***}p < 0.001$ (n = 4 animals for each group).

(H) Quantitative analysis of the percentage of BrdU-positive cells that express DCX in the hippocampi from 3- to 6-month-old WT and *Cbp*S436A-KI mice (n = 4 animals for each group).

Error bars represent SEM. See also Figure S2.

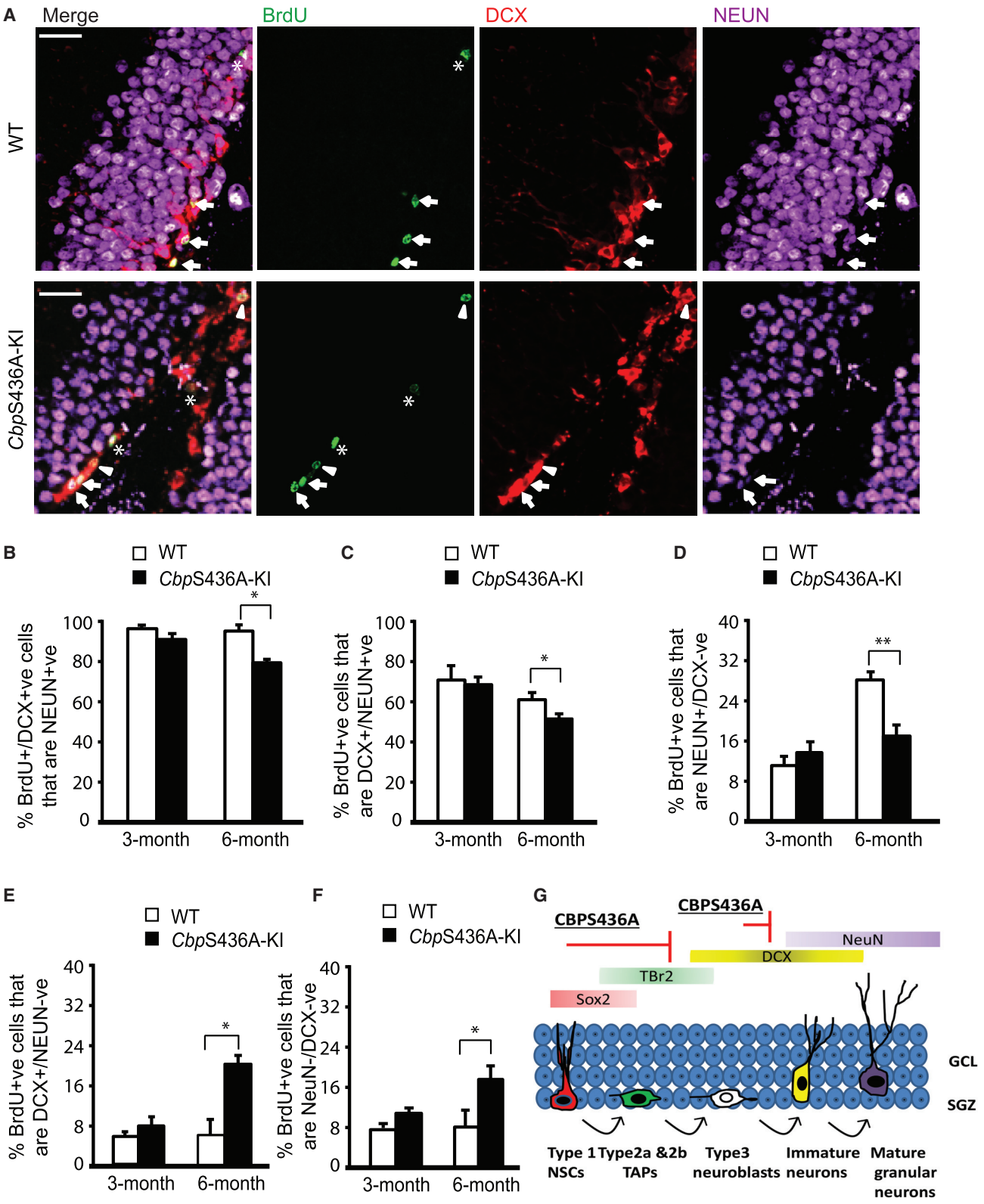

(legend on next page)

paradigm (Figure 3). Quantification of the proportion of BrdU/NEUN-positive neurons showed that rolipram treatment rescued the neurogenesis deficit observed in 6-month-old *Cbp*S436A-KI mice (Figures 6C and 6D). Further triple-labeling experiments (BrdU/DCX/NEUN) showed that the deficits from both neuronal differentiation (Figure 6F, the proportion of BrdU-positive cells that are negative for DCX and NEUN) and maturation (Figures 6G–6I, acquisition of NEUN-positive mature neurons in BrdU/DCX-positive immature cells) processes in 6-month-old *Cbp*S436A-KI mice were rescued by rolipram treatment. In addition, we also found that rolipram treatment increased the total number of Ki-67-positive proliferating cells in both WT and *Cbp*S436A-KI mice to the same extent (Figures S4C and S4D). Consistent with this, the proportion of BrdU-labeled DCX-positive cells was significantly increased by rolipram treatment in both WT and *Cbp*S436A-KI mice to the same extent (Figure S4E), while the total number of BrdU-positive cells was unchanged (Figure S4F). These results show that rolipram not only increases the proliferation and the population of BrdU-labeled DCX-positive cells regardless of genotype, but also prevents the neuronal differentiation and maturation deficits observed in *Cbp*S436A-KI mice.

We then asked whether rolipram treatment would restore the impaired fear memory of *Cbp*S436A-KI mice. Indeed, 21 days of rolipram treatment was capable of rescuing the impaired pre-exposure context fear memory (Figure 6J). Finally, co-immunoprecipitation assay showed that 14-day rolipram treatment rescued the impaired interaction between CBP and CREB in 6-month-old *Cbp*S436A-KI mice (Figures 6K–6L). Thus, these data support the concept that pS436-CBP is a compensatory mechanism in response to reduced pS133-CREB expression to maintain hippocampal neurogenesis, hippocampal-dependent fear memory, and the association of CBP with CREB in mature adult mice.

DISCUSSION

Our present data demonstrate four key events that are mediated by the aPKC-CBP pathway: (1) neurogenesis in young adult mice (3 months old) by, at least in part, preventing the death of newborn neurons; (2) maintenance of a stable rate of hippocampal neuronal differentiation and maturation in mature adult mice (6 months old); (3) formation of hippocampal-dependent fear memory and maintenance of spatial learning and memory in mature adult mice (6 months old); and (4) maintenance of the association of CBP with CREB in mature adult hippocampi (6 months old), when CREB activity/pS133-CREB is significantly reduced. Importantly, elevation of pS133-CREB expression in vivo rescues the impaired phenotypes at the cellular, behavioral, and molecular levels in mature adult *Cbp*S436A-KI mice where the aPKC-CBP pathway is deficient. Hence, our study strongly argues that the aPKC-CBP pathway is a homeostatic intrinsic mechanism that maintains a sustained rate of hippocampal neurogenesis and hippocampal-dependent memory in response to reduced CREB activity during early adulthood (3–6 months).

Originally, we identified the aPKC-CBP pathway as a pro-differentiation pathway during embryonic cerebral cortex development (Wang et al., 2010). Enriched neural developmental cues during cortex development converge on the aPKC-CBP pathway to promote the differentiation of embryonic NPCs into three neural cell lineages. Here, we ask a different question as to whether aPKC-mediated CBP phosphorylation/activation is a homeostatic signaling cascade that modulates adult hippocampal neurogenesis. Interestingly, recent research indicates that an early and dramatic decline in hippocampal neurogenesis during early adulthood (3–6 months) is primarily due to a decrease in neural progenitor proliferation and newborn neuron survival in the absence of any large changes in neuronal

Figure 3. Mature Adult Mice Lacking CBPS436 Phosphorylation Show Impaired Hippocampal Neuronal Maturation

Adult mice (6 months old) received BrdU (100 mg/kg) injections for 3 consecutive days, and were euthanized 12 days after the first BrdU injection.

(A) Confocal Images of coronal hippocampal dentate gyrus sections from 6-month-old WT and *Cbp*S436A-KI mice, stained for BrdU (green), DCX (red), and NEUN (purple). Arrows denote triple-labeled $BrdU^+/DCX^+/NEUN^+$ cells; arrowheads denote double-labeled $BrdU^+/DCX^+/NEUN^-$ cells; asterisks denote single-labeled $BrdU^+/DCX^-/NEUN^-$ cells. Scale bars, 20 μm.

(B–F) Quantitative analysis of the percentage of BrdU/DCX-positive cells that also express NEUN (B); the percentage of BrdU-positive cells that were positive for both NEUN and DCX (C); the percentage of BrdU-positive cells that were positive for NEUN but negative for DCX (D); the percentage of BrdU-positive cells that express DCX but not NEUN (E); and the percentage of BrdU-positive cells that were negative for both NEUN and DCX (F) in the hippocampi from 3- to 6-month-old WT and *Cbp*S436A-KI mice. $^*p < 0.05$, $^{**}p < 0.01$ (n = 4 animals for each group).

(G) Schematic representation showing that *Cbp*S436A mutation not only arrests the NPC development at SOX2 and/or $TBR2^+$ NSCs/TAPs but also inhibits neuronal maturation from DCX^+ cells to $NEUN^+$ mature neurons in 6-month-old adult mice. NSCs, neural stem cells; TAPs, transient amplifying progenitors.

Error bars represent SEM.

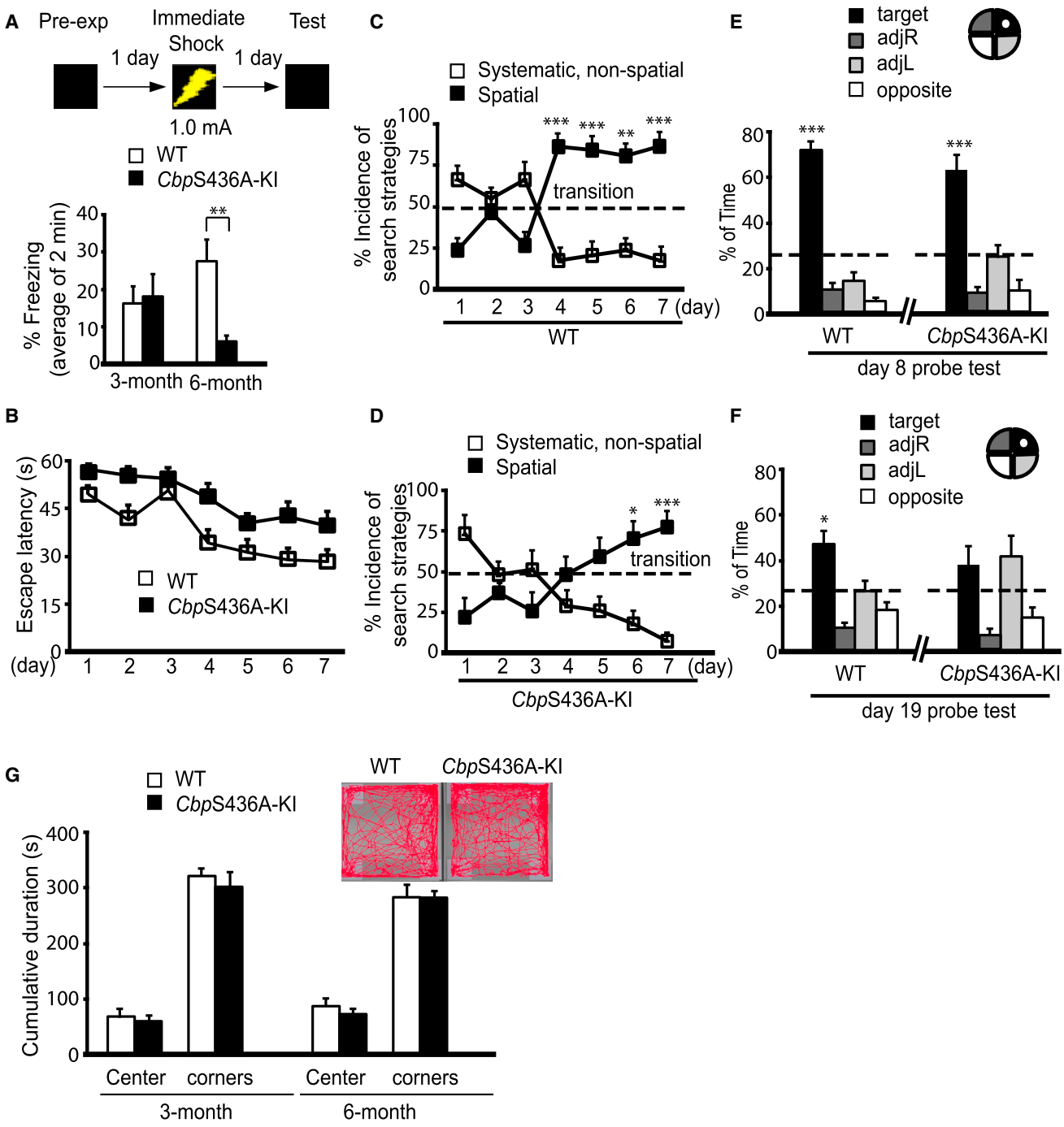

Figure 4. Mature Adult Mice Lacking CBPS436 Phosphorylation Display Impaired Pre-exposure Contextual Fear Memory and Deficits in Spatial Learning and Memory

(A) Both 3- and 6-month-old WT and *Cbp*S436-KI mice were pre-exposed to the conditioning context at day 1, and received an immediate shock (1.0 mA, 2 s) within the same context at day 2. Graph shows percentage of time spent freezing within the first 2 min when the mice were re-placed in the conditioning context at day 3 without shock $^{**}p < 0.01$ (n = 11 animals for each group).

(B–F) Six-month-old WT and *Cbp*S436A-KI mice were trained on the hidden-platform version of the Morris water maze (MWM) for 7 days. Early probe (day 8, 1 day after training) and late probe (day 19, 12 days after training) tests were performed on these mice by removing the submerged platform from the pool and leaving them to swim for a period of 60 s. (B) Acquisition of the platform location across a 7-day training session with latency to reach the platform as a measurement of learning. *Cbp*S436A-KI and WT groups had a comparable learning

(legend continued on next page)

differentiation rates (Kuipers et al., 2015). Thus, a sustained rate of neuronal differentiation may produce sufficient amounts of newborn neurons that can be functionally integrated into neural circuits to support increased memory during adulthood. In the present study, we found that the aPKC-CBP pathway is essential to maintain the stable rate of hippocampal neuronal differentiation and maturation during early adulthood development (3–6 months), suggesting its role as a homeostatic intrinsic mechanism in response to cellular changes during early adulthood to sustain functional neurogenesis, a key player in hippocampal-dependent memory formation.

In addition to phenotypic analyses, our study also provides insights into the molecular mechanisms that mediate the aPKC-CBP pathway in regulating hippocampal neurogenesis and hippocampal-dependent memory in an age-dependent manner. Previous work in liver cells shows that fully phosphorylated CBP at S436 eliminates the binding of CBP to CREB to regulate gluconeogenic gene expression (He et al., 2009), while we found that CBPS436 phosphorylation is required for CBP to bind to CREB in mature adult hippocampal extracts (6 months old) but not those of young adult mice (3 months old). The discrepancy between the hepatic and hippocampal tissues may be explained by the different CREB signals in the two tissue types. Specifically, CREB was constantly phosphorylated at S133 in hepatic tissue under the testing condition (He et al., 2009), while hippocampal tissues showed a significant reduction of pS133-CREB in mature adults (6 months old) regardless of the genotype. pS133-CREB is known to be a rate-limiting step in promoting the interaction between CREB and CBP (Parker et al., 1996). Our working model is that high levels of S133-phosphorylated CREB in young adult hippocampi play a dominant, stimulatory role in the regulation of the binding between CBP and CREB, whereas S436 phosphorylation in CBP is a compensatory regulator for the interaction between CBP and CREB in mature adult hippocampi when pS133-CREB is significantly reduced (Figure 7). This model is well supported by our data showing that aPKC activity was significantly enhanced in mature adult hippocampi where a significant reduction of pS133-CREB is evident. More interestingly, we observe that the activated form of CREB, pS133-CREB, is restrictively expressed in the hippocampal SGZ neurogenic region. Moreover, most of pS133-CREB-positive cells in the hippocampi are DCX-positive neuroblasts/newborn neurons, suggesting its role in the acquisition and maturation of DCX-positive cells. This idea has been explored in several previous studies (Herold et al., 2011; Merz et al., 2011; Nakagawa et al., 2002b). Importantly, we show here that the expression of pS133-CREB is robustly reduced in the adult hippocampi during early adulthood. We further demonstrate that elevation of CREB phosphorylation by rolipram treatment is able to rescue the hippocampal neuronal differentiation deficit and impaired pre-exposure fear memory, and restore diminished CBP binding to CREB in mature adult *Cbp*S436A-KI mice (6 months old). Together, these data suggest that the aPKC-CBP pathway is a compensatory signaling cascade that is activated in response to reduced CREB activity in mature adult hippocampi to sustain the interaction between CBP and CREB, potentially contributing to hippocampal neurogenesis and hippocampal-dependent fear memory.

Our behavioral work showed that the aPKC-CBP pathway is required for hippocampal-dependent fear memory formation in mature adult mice (6 months old) but not young adult mice (3 months old). This observation correlates well with the age-dependent functions of the aPKC-CBP pathway in maintaining hippocampal neuronal differentiation and maturation and CREB binding ability, suggesting that the aPKC-CBP/CREB signaling is key in the formation of hippocampal-dependent fear memory.

curve despite higher overall escape latency in *Cbp*S436A-KI mice (two-way ANOVA: main effect of genotypes $F(1,20) = 15.4$, $p < 0.001$; main effect of training day $F(6,120) = 10.95$, $p < 0.001$; genotype × training day interaction $F(6,120) = 0.77$, $p = 0.58$, $n = 22$). (C and D) Incidence of search strategies was analyzed using a fully automatic MWM visual algorithm. WT mice (C) were able to switch navigational search strategies from systematic to spatial search strategies by training day 4, while *Cbp*S436A-KI mice (D) exhibited a delayed transition from systematic to spatial search strategies at training day 6 (two-way ANOVA, WT: training day × strategy interaction, $F(6,66) = 12.2$, $p < 0.001$; post hoc multiple comparison, ***$p < 0.001$, **$p < 0.01$, $n = 12$; *Cbp*S436A-KI: training day × strategy interaction, $F(6,54) = 9.1$, $p < 0.001$; post hoc multiple comparison, ***$p < 0.001$, *$p < 0.05$, $n = 10$). Dashed line defines 50% incidence in the use of search strategies. (E) The percentage of time spent in four quadrant zones was analyzed at day 8 as a measurement of short-term memory (one-way ANOVA, WT: $F(3,44) = 131.2$, $p < 0.001$, target quadrant > all other quadrants, ***$p < 0.001$, $n = 12$; *Cbp*S436A-KI: $F(3,36) = 29$, $p < 0.001$, target quadrant > all other quadrants, ***$p < 0.001$, $n = 10$). (F) The percentage of time spent in four quadrant zones was analyzed at day 19 as a measurement of long-term memory (one-way ANOVA, WT: $F(3,44) = 11.78$, $p < 0.001$; target quadrant > all other quadrants, *$p < 0.05$, $n = 12$; *Cbp*S436A-KI: $F(3,36) = 8.3$, $p < 0.001$; for the target quadrant relative all other quadrants, not significant, $p > 0.05$, $n = 10$).

(G) The open field test was performed in an open box for 10 min. The cumulative time spent within the center and all four corners of the box was analyzed. Insets show representative traces of WT and *Cbp*S436A-KI mouse during the course of the open field test.

Error bars represent SEM. See also Figure S3.

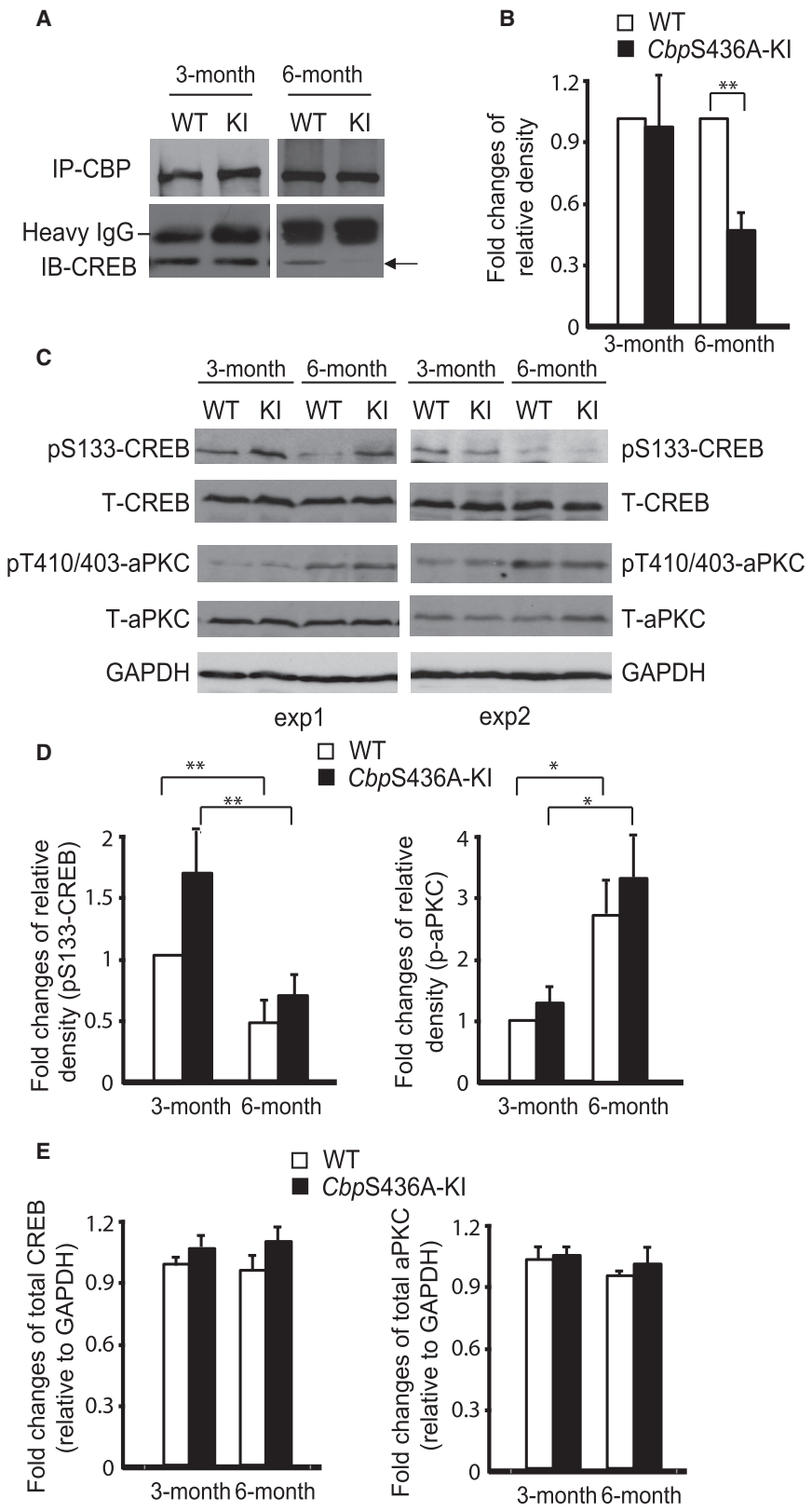

Figure 5. Mature Adult Mice Lacking CBPS436 Phosphorylation Display Impaired CBP Binding to CREB

(A) Co-immunoprecipitation analysis of the interaction between CBP and CREB in the hippocampus of WT and *Cbp*S436A-KI mice at 3 and 6 months. Hippocampal lysates were immunoprecipitated with a CBP antibody, washed, and blotted with the indicated antibody (n = 4 animals for each group). Arrow indicates CREB-expression band. IP, immunoprecipitation; IB, immunoblot; IgG, immunoglobulin G.

(B) Graph indicating the fold changes of the relative pulled-down CREB protein over the total CBP amounts, as determined by densitometry. $^{**}p < 0.01$ (n = 4 animals for each group).

(C) Western blot analysis for CREB phosphorylation at S133 and aPKC zeta/iota phosphorylation at T410/403 in hippocampal tissue extracts from 3- to 6-month-old WT and *Cbp*S436A-KI mice. Blots were re-probed for total CREB or aPKC, with GAPDH as loading control.

(D) Graphs show relative levels of phosphorylation of CREB and aPKC over total CREB and aPKC, respectively, normalized to samples from 3-month-old WT. $^{*}p < 0.05$, $^{**}p < 0.01$ (n = 4 animals for each group).

(E) Graphs show relative levels of total CREB and aPKC over GAPDH, normalized to one of the 3-month WT samples (n = 4 animals for each group).

Error bars represent SEM.

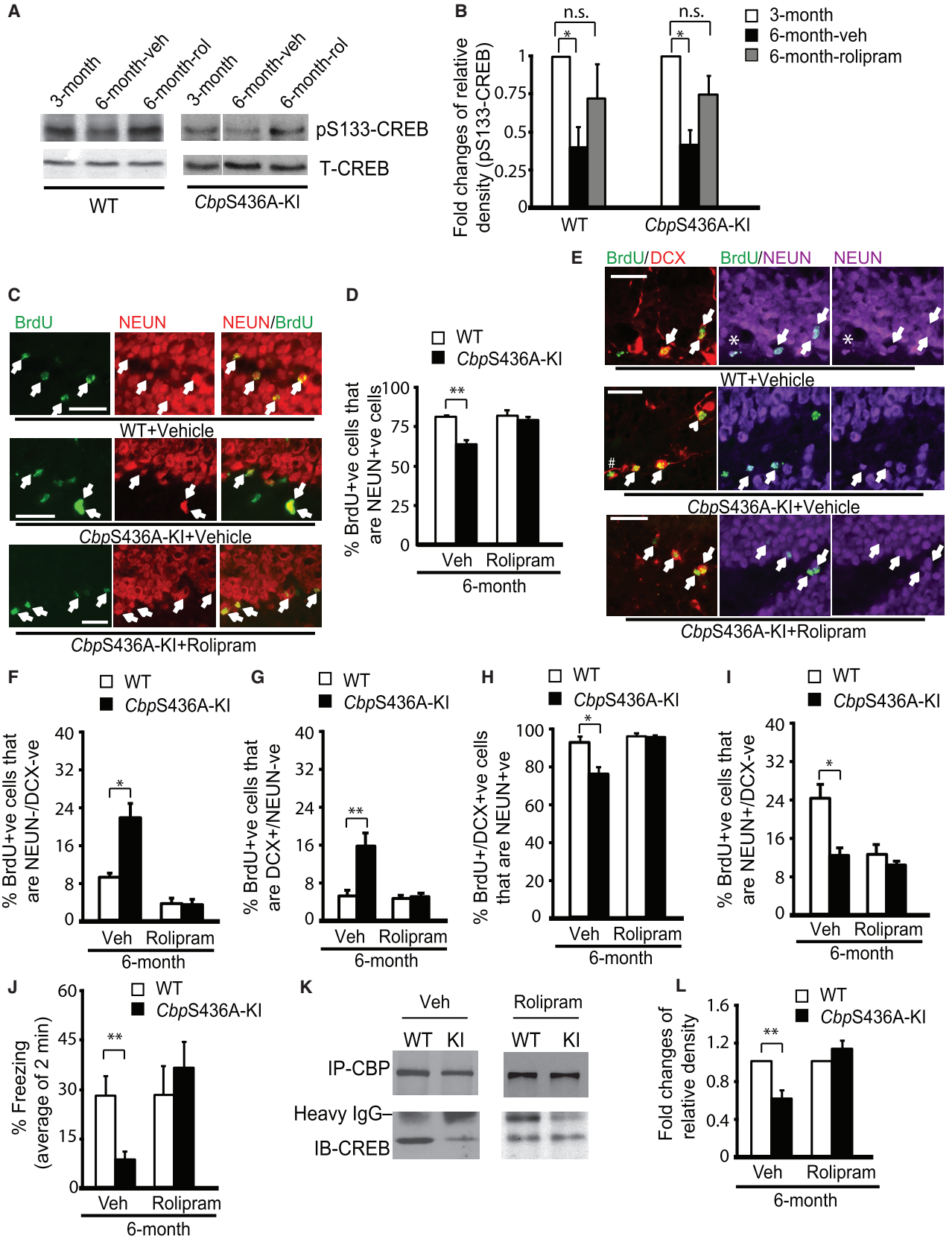

(legend on next page)

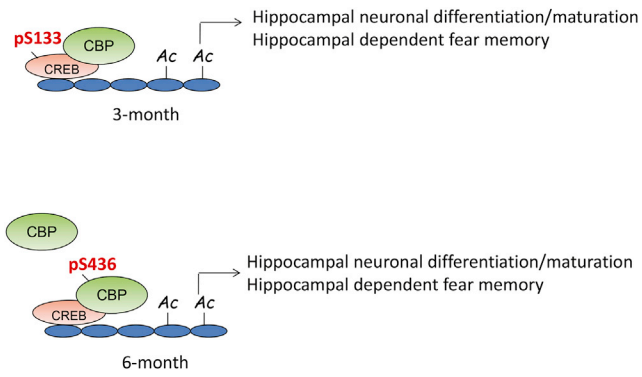

Figure 7. Working Model Depicting the Interaction between CBP and CREB

Highly phosphorylated CREB at S133 in young adult hippocampi (3 months old) plays a dominant role in the regulation of the interaction between CBP and CREB, whereas S436 phosphorylation in CBP is a compensatory regulator of CBP-CREB binding in mature adult hippocampi (6 months old) to promote hippocampal neuronal differentiation and maturation and hippocampal-dependent memory when pS133-CREB is significantly reduced.

This idea was also supported by a previous study showing that *Cbp*^{kix} mutant mice that lack the interaction with CREB have reduced hippocampal-dependent fear memory associated with decreased CREB-mediated gene transcription (Wood et al., 2006). In addition, our comprehensive analysis of the MWM task indicated that the aPKC-CBP pathway is required for spatial learning and long-term spatial memory in mature adult mice. The mice lacking the aPKC-CBP pathway exhibit a delayed acquisition of spatial search strategies, showing impaired spatial learning, as well as the disruption of long-term spatial memory. These results are very intriguing, as previous findings from other *Cbp* mutants generated by modifying endogenous *Cbp* gene alleles (Alarcón et al., 2004; Oike et al., 1999) show normal spatial memory measured by the MWM task. This strongly argues that CBP phosphorylation at Ser436 is a signaling cascade that specifically fine-tunes spatial memory by modulating adult hippocampal neurogenesis in an age-dependent manner.

Altogether, our findings support a concept that the aPKC-CBP pathway is a homeostatic signaling cascade that maintains functional hippocampal neurogenesis and forms hippocampal-dependent memory in response to cellular/molecular changes during early adulthood. Disruption of the homeostatic signaling may be involved in the pathogenesis of neurodegenerative disease such as Alzheimer's disease.

EXPERIMENTAL PROCEDURES

Animals and Drug Treatment

All animal use was approved by the Animal Care Committees of the Hospital for Sick Children and the University of Ottawa in accordance with the Canadian Council of Animal Care policies. *Cbp*S436A mice (Zhou et al., 2004) were maintained on a 12-hr light/12-hr dark cycle with ad libitum access to food and water. Detailed information regarding animals and drug treatment is provided in Supplemental Experimental Procedures.

Figure 6. Rolipram, a PDE4 Inhibitor, Rescues Neuronal Differentiation Deficit and Impaired Fear Memory, and Restores the Association between CBP and CREB in Mature Adult *Cbp*S436A-KI Mice

Six-month-old mice received rolipram intraperitoneally or vehicle (veh) for 14 days, and were euthanized for western blot and immunostaining analyses.

(A) Western blot analysis for CREB phosphorylation at S133 in hippocampal extracts from 3-to 6-month-old WT and *Cbp*S436A-KI mice. Blots were reprobed for total CREB as loading controls.

(B) Graph shows the relative level of phosphorylation of CREB over total CREB. *$p < 0.05$ ($n = 3$ animals for each group). n.s., not significant.

(C and E) Fluorescence images of hippocampal sections from 6-month-old WT and *Cbp*S436A-KI mice in the presence of rolipram or vehicle, (C) stained for BrdU (green) and NEUN (red), arrows denote BrdU/NEUN-positive neurons; (E) stained for BrdU (green), DCX (red), and NEUN (purple), arrows denote triple-labeled BrdU$^+$/DCX$^+$/NEUN$^+$ cells, arrowhead denotes BrdU$^+$/DCX$^+$/NEUN$^-$ cells, asterisks denote BrdU$^+$/DCX$^-$/NEUN$^+$ cells, and hash denotes BrdU$^+$/DCX$^-$/NEUN$^-$ cells. Scale bars, 25 μm (C) and 20 μm (E).

(D and F–I) Quantitative analysis of the percentage of BrdU-positive cells that express NEUN (D), the percentage of BrdU-positive cells that were negative for both NEUN and DCX (F), the percentage of BrdU-positive cells that express DCX but not NEUN (G), the percentage of BrdU-positive, DCX-positive cells that also express NEUN (H), and the percentage of BrdU-positive cells that were positive for NEUN but negative for DCX (I) in the hippocampi from WT and *Cbp*S436A-KI mice. *$p < 0.05$, **$p < 0.01$ ($n = 4$ animals for each group).

(J) Percentage of time spent freezing in the context that was pre-exposed to the mice 2 days prior, and together with an immediate shock 1 day before, following 3-week rolipram (or vehicle) treatment in 6-month-old WT and *Cbp*S436-KI mice. **$p < 0.01$ ($n = 11$ animals for each group).

(K and L) Co-immunoprecipitation analysis of the interaction between CBP and CREB in the hippocampus of 6-month-old WT and *Cbp*S436A-KI mice upon rolipram or vehicle treatment. IP, immunoprecipitation; IB, immunoblot; IgG, immunoglobulin G. The graph (L) indicates the fold changes of the relative pulled-down CREB protein over the total CBP amounts. **$p < 0.01$ ($n = 3$ animals for each group) Veh, vehicle.

Error bars represent SEM. See also Figure S4.

BrdU Labeling

In one set of experiments, mice were injected intraperitoneally with 100 mg/kg BrdU (Sigma-Aldrich) once and then euthanized 24 hr later. In a second set of experiments, mice were injected intraperitoneally with 100 mg/kg BrdU once daily for 3 days. These mice were euthanized 12 days after the first BrdU injection. In a third set of experiments, mice were injected intraperitoneally with 60 mg/kg BrdU four times at 3-hr intervals (Morshead et al., 1998), and euthanized 30 days later. Detailed information on tissue processing is provided in Supplemental Experimental Procedures.

Immunohistochemistry, Microscopy, and Quantification

Detailed information is provided in Supplemental Experimental Procedures.

Co-immunoprecipitation, Western Blot Analysis, and Densitometry

Hippocampal tissues were homogenized and lysed in lysis buffer, as detailed in Supplemental Experimental Procedures.

Context Pre-exposure Fear Conditioning, Morris Water Maze Task, and Open Field Test

For context pre-exposure fear conditioning, mice were trained as described previously (Frankland et al., 2004), as detailed in Supplemental Experimental Procedures. The MWM task and open field test were performed by the Behavioral Core Facility at the University of Ottawa. Detailed information is provided in Supplemental Experimental Procedures.

Antibodies

Detailed information is provided in Supplemental Experimental Procedures.

Statistics

Statistical analyses were performed with a two-tailed Student's t test or ANOVA with Sidak's multiple comparison post hoc analysis, unless otherwise indicated. Error bars indicate the SEM.

SUPPLEMENTAL INFORMATION

Supplemental Information includes Supplemental Experimental Procedures and four figures and can be found with this article online at http://dx.doi.org/10.1016/j.stemcr.2016.08.007.

AUTHOR CONTRIBUTIONS

A.G. and K.H. equally performed experiments, analyzed data, and contributed to paper writing; Y.N. performed fear memory experiments; Y.N. and P.F. contributed to fear memory experimental design, data analysis, and interpretation; M.S. and G.I.C. performed experiments; S.B. contributed to search strategies analysis; D.L. contributed to MWM experimental design, data analysis, and interpretation; L.H. and F.W. generated *Cbp*S436A knockin mouse strain; J.W. designed and performed experiments, analyzed and interpreted data, and wrote the paper.

ACKNOWLEDGMENTS

We are indebted to Dr. Freda Miller who provided very strong support for the work presented herein. This work was supported by the J.P. Bickell Foundation, Ottawa Hospital Foundation, and NSERC Discovery Grant (RGPIN-2016-05656) to J.W., and CIHR (FDN143227) to P.F. P.F. is a Canada Research Chair. We thank Dennis Aquino for mouse colony assistance, and Mirela Hasu and Christine Luckhart of the behavioral core for technical assistance.

Received: July 27, 2015
Revised: August 10, 2016
Accepted: August 11, 2016
Published: September 8, 2016

REFERENCES

Alarcón, J.M., Malleret, G., Touzani, K., Vronskaya, S., Ishii, S., Kandel, E.R., and Barco, A. (2004). Chromatin acetylation, memory, and LTP are impaired in CBP+/- mice: a model for the cognitive deficit in Rubinstein-Taybi syndrome and its amelioration. Neuron *42*, 947–959.

Cancino, G.I., Yiu, A.P., Fatt, M.P., Dugani, C.B., Flores, E.R., Frankland, P.W., Josselyn, S.A., Miller, F.D., and Kaplan, D.R. (2013). p63 regulates adult neural precursor and newly born neuron survival to control hippocampal-dependent behavior. J. Neurosci. *42*, 12569–12585.

Deng, W., Aimone, J.B., and Gage, F.H. (2010). New neurons and new memories: how does adult hippocampal neurogenesis affect learning and memory? Nat. Rev. Neurosci. *11*, 339–350.

Dupret, D., Fabre, A., Döbrössy, M.D., Panatier, A., Rodríguez, J.J., Lamarque, S., Lemaire, V., Oliet, S.H., Piazza, P.V., and Abrous, D.N. (2007). Spatial learning depends on both the addition and removal of new hippocampal neurons. PLoS Biol. *5*, e214.

Fanselow, M.S. (2000). Contextual fear, gestalt memories, and the hippocampus Behav. Brain Res. *10*, 73–81.

Fatt, M., Hsu, K., He, L., Wondisford, F., Miller, F.D., Kaplan, D.R., and Wang, J. (2015). Metformin acts on two different molecular pathways to enhance adult neural precursor proliferation/self-renewal and differentiation. Stem Cell Rep. *5*, 1–8.

Frankland, P.W., Josselyn, S.A., Anagnostaras, S.G., Kogan, J.H., Takahashi, E., and Silva, A.J. (2004). Consolidation of CS and US representations in associative fear conditioning. Hippocampus *14*, 557–569.

Granger, M.W., Franko, B., Taylor, M.W., Messier, C., St George-Hyslop, P., and Bennett, S.A. (2016). A TgCRND8 mouse model of Alzheimer's disease exhibits sexual dimorphisms in behavioral indices of cognitive reserve. J. Alzheimers Dis. *51*, 757–773.

He, L., Sabet, A., Djedjos, S., Miller, R., Sun, X., Hussain, M.A., Radovick, S., and Wondisford, F.E. (2009). Metformin and insulin suppress hepatic gluconeogenesis through phosphorylation of CREB binding protein. Cell *137*, 635–646.

Herold, S., Jagasia, R., Merz, K., Wassmer, K., and Lie, D.C. (2011). CREB signalling regulates early survival, neuronal gene expression and morphological development in adult subventricular zone neurogenesis. Mol. Cell. Neurosci. *46*, 79–88.

Imayoshi, I., Sakamoto, M., Ohtsuka, T., Takao, K., Miyakawa, T., Yamaguchi, M., Mori, K., Ikeda, T., Itohara, S., and Kageyama, R. (2008). Roles of continuous neurogenesis in the structural and functional integrity of the adult forebrain. Nat. Neurosci. *11*, 1153–1161.

Kee, N., Teixeira, C.M., Wang, A.H., and Frankland, P.W. (2007). Preferential incorporation of adult-generated granule cells into spatial memory networks in the dentate gyrus. Nat. Neurosci. *10*, 355–362.

Kuipers, S.D., Schroeder, J.E., and Trentani, A. (2015). Changes in hippocampal neurogenesis throughout early development. Neurobiol. Aging *36*, 365e379.

Lopez-Atalaya, J.P., Ciccarelli, A., Viosca, J., Valor, L.M., Jimenez-Minchan, M., Canals, S., Giustetto, M., and Barco, A. (2011). CBP is required for environmental enrichment-induced neurogenesis and cognitive enhancement. EMBO. J. *30*, 4287–4298.

Matus-Amat, P., Higgins, E.A., Barrientos, R.M., and Rudy, J.W. (2004). The role of the dorsal hippocampus in the acquisition and retrieval of context memory representations. J. Neurosci. *24*, 2431–2439.

Merz, K., Herold, S., and Lie, D.C. (2011). CREB in adult neurogenesis—master and partner in the development of adult-born neurons? Eur. J. Neurosci. *33*, 1078–1086.

Mizuno, M., Yamada, K., Maekawa, N., Saito, K., Seishima, M., and Nabeshima, T. (2002). CREB phosphorylation as a molecular marker of memory processing in the hippocampus for spatial learning. Behav. Brain Res. *133*, 135–141.

Morshead, C.M., Craig, C.G., and van der Kooy, D. (1998). In vivo clonal analyses reveal the properties of endogenous neural stem cell proliferation in the adult mammalian forebrain. Development *125*, 2251–2261.

Mu, Y., and Gage, F.H. (2011). Adult hippocampal neurogenesis and its role in Alzheimer's disease. Mol. Neurodegener. *6*, 85.

Ming, G.L., and Song, H. (2011). Adult neurogenesis in the mammalian brain: significant answers and significant questions. Neuron *70*, 687–702.

Nakagawa, S., Kim, J.E., Lee, R., Malberg, J.E., Chen, J., Steffen, C., Zhang, Y.J., Nestler, E.J., and Duman, R.S. (2002a). Regulation of neurogenesis in adult mouse hippocampus by cAMP and the cAMP response element-binding protein. J. Neurosci. *22*, 3673–3682.

Nakagawa, S., Kim, J.E., Lee, R., Chen, J., Fujioka, T., Malberg, J., Tsuji, S., and Duman, R.S. (2002b). Localization of phosphorylated cAMP response element-binding protein in immature neurons of adult Hippocampus. J. Neurosci. *22*, 9868–9876.

Oike, Y., Hata, A., Mamiya, T., Kaname, T., Noda, Y., Suzuki, M., Yasue, H., Nabeshima, T., Araki, K., and Yamamura, K. (1999). Truncated CBP protein leads to classical Rubinstein-Taybi syndrome phenotypes in mice: implications for a dominant-negative mechanism. Hum. Mol. Genet. *8*, 387–396.

Palmer, T.D., Takahashi, J., and Gage, F.H. (1997). The adult rat hippocampus contains primordial neural stem cells. Mol. Cell. Neurosci. *8*, 389–404.

Parker, D., Ferreri, K., Nakajima, T., LaMorte, V.J., Evans, R., Koerber, S.C., Hoeger, C., and Montminy, M.R. (1996). Phosphorylation of CREB at Ser-133 induces complex formation with CREB-binding protein via a direct mechanism. Mol. Cell. Biol. *16*, 694–703.

Rudy, J.W., Huff, N.C., and Matus-Amat, P. (2004). Understanding contextual fear conditioning: insights from a two-process model. Neurosci. Biobehav. Rev. *28*, 675–685.

Sahay, A., Scobie, K.N., Hill, A.S., O'Carroll, C.M., Kheirbek, M.A., Burghardt, N.S., Fenton, A.A., Dranovsky, A., and Hen, R. (2011). Increasing adult hippocampal neurogenesis is sufficient to improve pattern separation. Nature *472*, 466–470.

Saxe, M.D., Battaglia, F., Wang, J.W., Malleret, G., David, D.J., Monckton, J.E., Garcia, A.D., Sofroniew, M.V., Kandel, E.R., Santarelli, L., et al. (2006). Ablation of hippocampal neurogenesis impairs contextual fear conditioning and synaptic plasticity in the dentate gyrus. Proc. Natl. Acad. Sci. USA *103*, 17501–17506.

Silva, A.J., Kogan, J.H., Frankland, P.W., and Kida, S. (1998). Creb and memory. Annu. Rev. Neurosci. *21*, 127–148.

Shih, H.M., Goldman, P.S., BeMaggio, A.J., Holleggerg, S.M., Goodman, R.H., and Hoekstra, M.F. (1996). A positive genetic selection for disrupting protein-protein interactions: identification of CREB mutations that prevent association with the coactivator CBP. Proc. Natl. Acad. Sci. USA *93*, 13896–13901.

Toni, N., Laplagne, D.A., Zhao, C., Lombardi, G., Ribak, C.E., Gage, F.H., and Schinder, A.F. (2008). Neurons born in the adult dentate gyrus form functional synapses with target cells. Nat. Neurosci. *11*, 901–907.

Tsui, D., Voronova, A., Gallagher, D., Kaplan, D.R., Miller, F.D., and Wang, J. (2014). CBP regulates the differentiation of interneurons from ventral forebrain neural precursors during murine development. Dev. Biol. *385*, 230–241.

Wang, J., Weaver, I.C.G., Gauthier-Fisher, A.S., Wang, H., He, L., Yeomans, J., Wondisford, F., Kaplan, D.R., and Miller, F.D. (2010). CBP histone acetyltransferase activity regulates embryonic neural differentiation in the normal and Rubinstein-Taybi syndrome brain. Dev. Cell *18*, 114–125.

Wang, J., Gallagher, D., DeVito, L., Cancino, I., Tsui, D., He, L., Keller, G.M., Frankland, P.W., Kaplan, D.R., and Miller, F.D. (2012). Metformin activates atypical PKC-CBP pathway to promote neurogenesis and enhance spatial memory formation. Cell Stem Cell *11*, 23–35.

Winner, B., Kohl, Z., and Gage, F.H. (2011). Neurodegenerative disease and adult neurogenesis. Eur. J. Neurosci. *33*, 1139–1151.

Wood, M.A., Attner, M.A., Oliveira, A.M.M., Brindle, P.K., and Abel, T.A. (2006). A transcription factor-binding domain of the coactivator CBP is essential for long-term memory and the expression of specific target genes. Learn. Mem. *13*, 609–617.

Zhou, X.Y., Shibusawa, N., Naik, K., Porras, D., Temple, K., Ou, H., Kaihara, K., Roe, M.W., Brady, M.J., and Wondisford, F.E. (2004). Insulin regulation of hepatic gluconeogenesis through phosphorylation of CREB-binding protein. Nat. Med. *10*, 633–637.

Zhao, C., Deng, W., and Gage, F.H. (2008). Mechanisms and functional implications of adult neurogenesis. Cell *132*, 645–660.

Stem Cell Reports, Volume *7*

Supplemental Information

The aPKC-CBP Pathway Regulates Adult Hippocampal Neurogenesis in an Age-Dependent Manner

Ayden Gouveia, Karolynn Hsu, Yosuke Niibori, Matthew Seegobin, Gonzalo I. Cancino, Ling He, Fredric E. Wondisford, Steffany Bennett, Diane Lagace, Paul W. Frankland, and Jing Wang

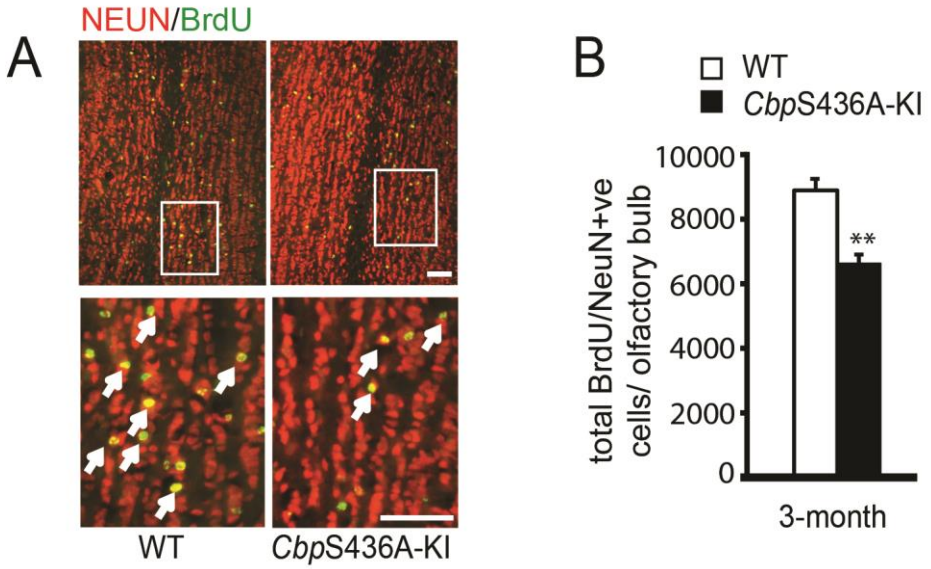

Figure S1. Young adult mice (3 months) lacking CBPS436 phosphorylation show a reduction in adult olfactory bulb neurogenesis, related to Figure 1. (A) Fluorescence photomicrographs of coronal olfactory bulb (OB) sections from 3-month old WT and *Cbp*S436A-KI mice 30 days after BrdU injection. Sections were stained for BrdU (green) and NEUN (red). Scale bar =20 μm. (B) Quantitative analysis of the total number of BrdU-positive, NEUN-positive newborn neurons, determined from sections as shown in (A), in OB from WT and *Cbp*S436A-KI mice (3-month old). **$p < 0.01$ ($n = 3$ for each group).

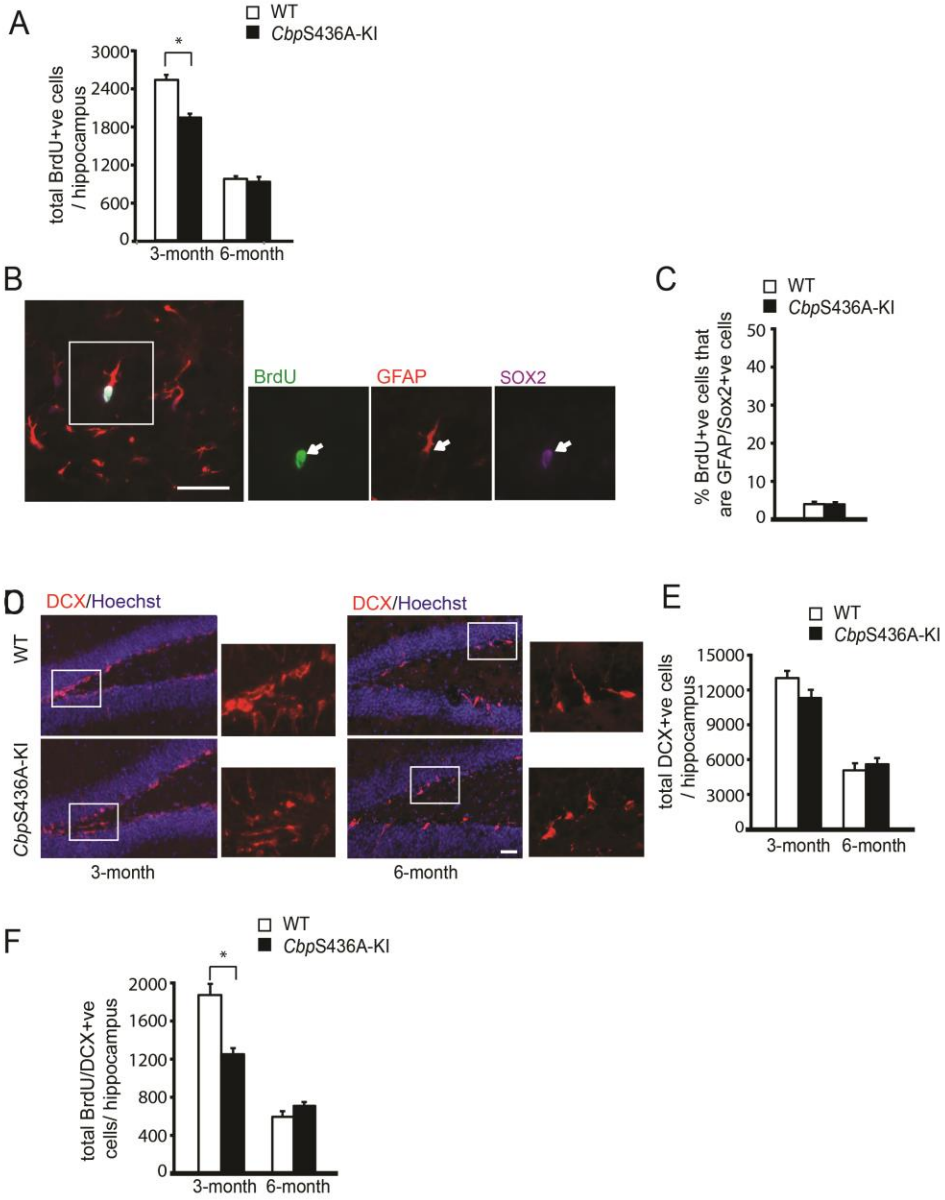

Figure S2. Total number of BrdU positive cells was reduced in 3 months but not in 6 months *Cbp*S436A-KI mice 12 days after BrdU injections, related to Figure 2A. (A)Quantitative analysis of the total number of BrdU-positive cells in the hippocampi from WT and *Cbp*S436A-KI mice at the age of 3 and 6 months. (n =5-7 animals for each group). **The proportion of BrdU labelled GFAP/Sox2 positive type I radial glial cells was not changed in mature adult *Cbp*S436A-KI mice, related to Figure 2E-F. (**B**)** photomicrographs of coronal hippocampal sections from 6-month-old *Cbp*S436A KI mice, sacrificed 12 days after the first BrdU injections. Sections were stained for BrdU (green), GFAP (red) and SOX2 (purple). Scale bar =25µm. (C) Quantitative analysis of the percentage of BrdU-positive cells that are also positive for GFAP and Sox2 in the hippocampi from WT and *Cbp*S436A-KI mice at the age of 6 months. (n =3-4 animals for each group). **Total number of DCX positive cells was not changed in *Cbp*S436A-KI mice, while the number of BrdU-colabeled DCX positive cells was significantly reduced at 3 months *Cbp*S436A-KI mice, related to Figure 2G-H.** (D) Fluorescence photomicrographs of coronal hippocampal dentate gyrus sections from 3 months and 6 months WT (upper panels) and *Cbp*S436A-KI (lower panels) mice. Sections were stained for doublecortin (DCX) (red) and counter-stained for Hoechst 33342 (blue). Boxed areas were shown at higher magnification on the right. Scale bar=25µm. (E) Quantitative analysis of the total number of DCX-positive cells in the hippocampi from WT and *Cbp*S436A-KI mice at the age of 3 months and 6 months. (n = 4 animals for each group). (F) Quantitative analysis of the total number of BrdU positive, DCX-positive cells in the hippocampi from both 3 and 6 months WT and *Cbp*S436A-KI mice 12 days following BrdU injections (n = 5-7 animals for each group).

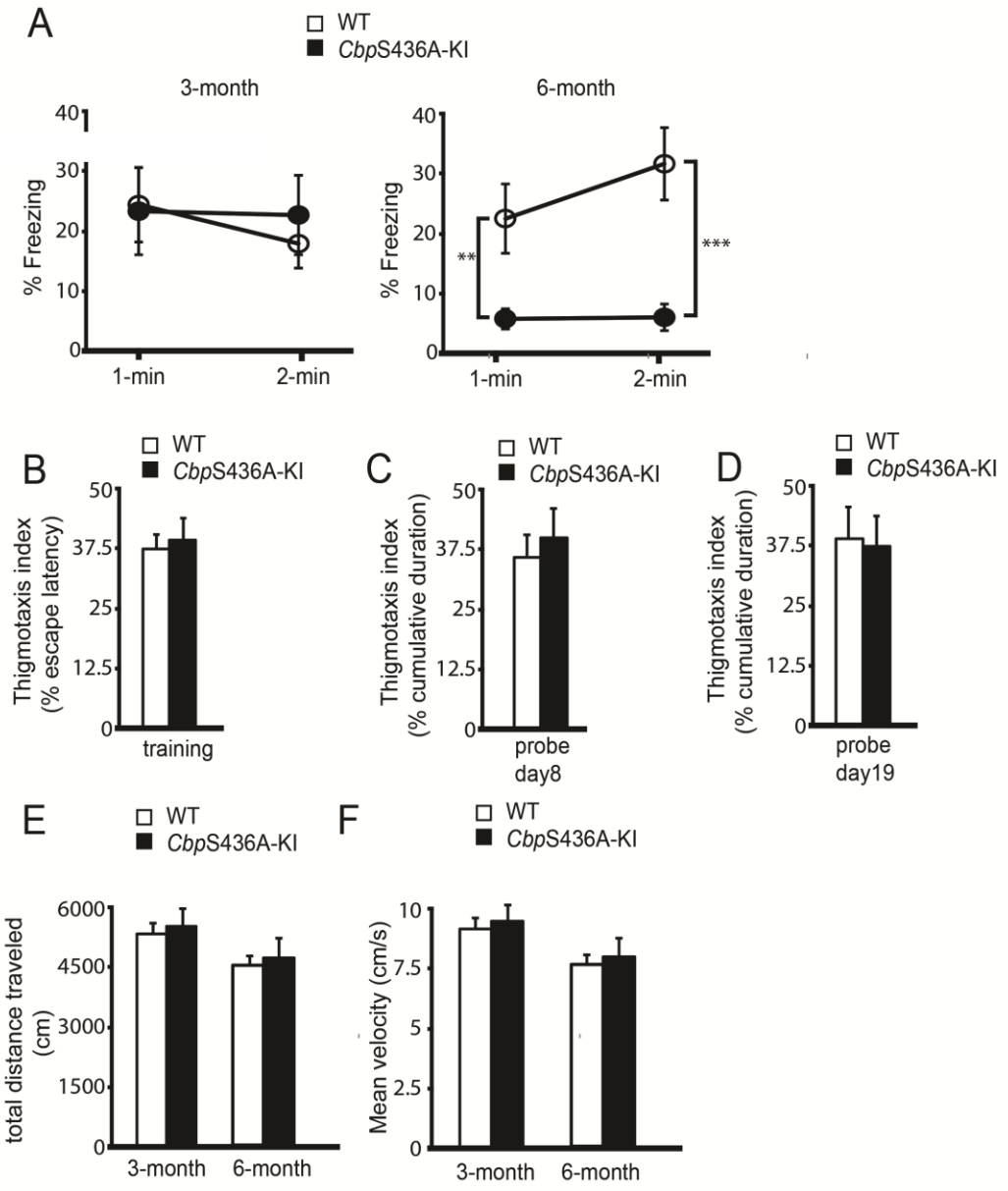

Figure S3. Mature adult mice (6 months) lacking CBP S436 phosphorylation show impaired pre-exposure contexture fear memory, related to Figure 4A.(A) Percentage of the time spent freezing in the context within each min for 3 and 6 months WT and *Cbp*S436A-KI mice. ** $p<0.01$; *** $p<0.001$. **Mature adult mice (6 months) lacking CBP S436 phosphorylation show the same thigmotaxis as their wild type littermates, related to Figure4B-F.** (B-D) Percentage of thigmotaxis were assessed for WT and *Cbp*S436A-KI mice during training (B), early (day8, C) and late probe (day 19, D) tests. **Mature adult mice (6 months) lacking CBP S436 phosphorylation show normal general motor activities, related to Figure4G.** (E) Analysis of the total distance travelled during the open field test for WT and *Cbp*S436A-KI mice at the age of 3 and 6 months. (F) Analysis of the mean velocity during the 10-minutes of movement for WT and *Cbp*S436A-KI mice at the age of 3 and 6 months.

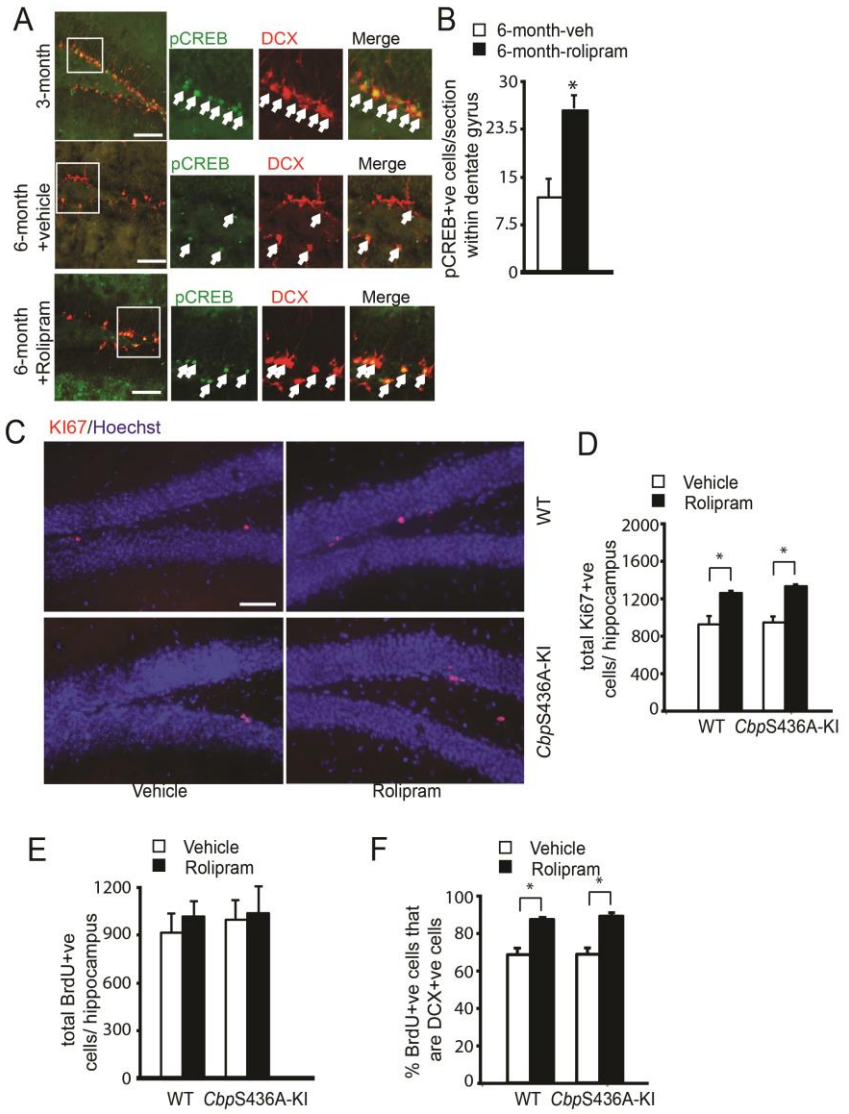

Figure S4. Rolipram treatment significantly increased the number of pS133-CREB positive cells in the 6-month-old hippocampal SGZ, related to Figure 6A-B. (A) Fluorescence photomicrographs of coronal hippocampal dentate gyrus sections from 3- and 6-month-old WT mice in the presence of rolipram or vehicle. Sections were stained for p-CREB (green), DCX (red). Arrows denote double labelled pS133-CREB/DCX positive cells Scale bar = 50 μm. (B) Quantitative analysis of the number of pS133-CREB positive cells in the 6-month-old hippocampal SGZ in the presence of rolipram or vehicle regardless of genotypes, determined from sections as shown in (A). *$p < 0.05$; veh: vehicle, n =4 animals for each group. **Rolipram treatment significantly increased total number of KI67 positive proliferating cells in both WT and *Cbp*S436A-KI mice, related to Figure 6C-I** (C) Fluorescence photomicrographs of coronal hippocampal dentate gyrus sections from 6 months WT (upper panels) and *Cbp*S436A-KI (lower panels) mice in the absence (left panels) and presence of rolipram (right panels). Sections were stained for KI67 (red) and counter-stained for Hoechst 33342 (blue). Scale bar=50μm. (D) Quantitative analysis of the total number of Ki67-positive cells in the hippocampi from WT and *Cbp*S436A-KI mice at the age of 6 months in the absence and presence of rolipram. (n = 4 animals for each group). **Rolipram treatment significantly increased the proportion of BrdU labelled DCX positive cells in both WT and *Cbp*S436A-KI mice, related to Figure 6E.(E)**Quantitative analysis of the total number of BrdU-positive cells in the hippocampi from WT and *Cbp*S436A-KI mice at the age of 6 months in the absence and presence of rolipram. (n = 4 animals for each group). (F) Quantitative analysis of the proportion of BrdU-positive cells that are positive for DCX in the hippocampi from WT and *Cbp*S436A-KI mice at the age of 6 months in the absence and presence of rolipram. (n = 4 animals for each group).

Supplemental Experimental Procedures:

Animals and drug treatment

Only wild type (WT) and homozygous (*Cbp*S436A-KI) mice were used as experimental mice and heterozygous of *Cbp*S436A were used for breeding. For rolipram treatment, mice were given saline containing 2% DMSO as a control (vehicle) or rolipram (1.25 mg/kg, i.p; Sigma, St. Louis, MO) in saline containing 2% DMSO daily for 14 or 21 days.

BrdU labeling

Following the three sets of BrdU-chasing experiments, the mice were sacrificed by a lethal dose of pentobarbital and perfused transcardially with PBS and 4% paraformaldehyde. Brains were postfixed, cryoprotected and cryosectioned at 20 μm and 14 μm for hippocampus and olfactory bulb, respectively. Every tenth hippocampal section was analyzed immunohistochemically for BrdU, NEUN, DCX, SOX2, GFAP and TBR2 as previously described (Wojtowicz et al., 2006).

Immunohistochemistry, microscopy, and quantification

Immunostaining of brain sections was performed as previously described (Wang et al., 2012). Sections were post-fixed with 4% PFA, blocked and permeabilized with 5% BSA and 0.3% Triton-X, and then sections were incubated with primary antibodies at 4ºC overnight, with secondary antibodies at room temperature for 1 hour, counterstained with Hoechst 33343 (1:2000, Sigma-Aldrich) and mounted using GelTol (Fisher). For BrdU colabelling with DCX, sections were first immunostained with anti-DCX followed by an Alexa Fluor 555-conjugated donkey anti-goat secondary antibody. Following that, the same sections were incubated in 2 N HCl at 45°C for 30 min, rinsed in PBS, incubated in rat anti-BrdU antibody at 4°C overnight,

and finally treated with Alexa 488 donkey anti-rat antibody for 1 hour. For BrdU colabelling with NEUN, TBR2, GFAP or SOX2, sections were incubated in 1 N HCl at 60°C for 30 min, rinsed in PBS, incubated in rat anti-BrdU antibody at 4°C overnight, in Alexa 488 donkey anti-rat antibody for 1 hour and then sequentially immunostained with anti-NEUN, anti-TBR2, anti-GFAP or anti-SOX2 followed by Alexa Fluor -conjugated secondary antibodies.

Digital image acquisition was performed using either a Zeiss Axioplan 2 fluorescent microscopy with Zeiss Axiovision software that contains z-axis capability, or a Zeiss LSM 510 confocal microscopy using Zeiss Zen Pro software V2.0 (Oberkochen, Germany). 10-15 images were captured in the Z-axis per section at a maximum of 1um apart and processed as an optical stack of 10-15 scanned slices for quantification.

For quantification, positive cells were quantified using a modified stereological method that have been extensively used (Eisch et al., 2000, Gould et al., 1999, Malberg et al., 2000, Olariu et al, 2007, Wang, et al, 2012, West et al., 1991). We exhaustively quantified every positive cell within dentate gyrus region including SGZ, GCL and hilus. Thus we used an area sampling fraction of 1 as is commonly utilized for counting rare populations of cells (Jayatissa et al., 2009, Mouton et al., 2002) since the raw counts for the numbers of positive cells were low according to disector/fractionator standards (Guillery, et al., 1997; Pakkenberg, et al., 1988; West, et al., 1990) and the cells are not evenly distributed within the dentate gyrus. Given recent work suggesting the absence of lost caps in perfusion fixed tissue and potential bias that can occur with traditional use of guard zones (Carlo, et al., 2011; Gardella, et al., 2003; Miller, et al., 2014), we did not employ a guard zone and used the same method to quantify both wild type and knock-in mice brain sections. We sampled 1 in every 10 sections throughout the septotemporal axis of the hippocampal structure (-1.3 mm to -3.70 mm relative to bregma referring to the

rostral-caudal coordinates) by an examiner that was blind to group assignments. Since the section sampling fraction was 1/10, the resulting raw count for each region was multiplied by 10 to obtain an estimate of the total number of cells per dentate gyrus.

Co-immunoprecipitation

Hippocampal tissues were homogenised and lysed in lysis buffer (25mM Tris, pH=7.4, 10mM NaCl, 2mM EDTA, 1mM EGTA, 0.5% Triton-100, 10% glycerol) containing 1mM PMSF, 1mM sodium orthovanadate, 20mM sodium fluoride, 10 μg/ml aprotinin and 10 μg/ml leupeptin. The extractions were sonicated 3 times with 5 seconds pulses at 1 minute intervals. Then, 1 mg protein lysate from each sample was incubated with 50 ul protein A conjugated magnetic beads and 3 ug anti-CBP antibody or normal rabbit IgG antibody at 4ºC overnight. Following that, the magnetic beads were rinsed 3 times with lysis buffer, boiled with sample buffer, and loaded on a 5-15% gradient SDS-PAGE gel.

Western blot analysis and densitometry

Hippocampal tissues were lysed in lysis buffer (25 mM Tris, pH=7.4, 10mM NaCl, 2mM EDTA, 1mM EGTA 0.5% Triton-100, 10% glycerol) containing 1 mM PMSF, 1 mM sodium orthovanadate, 20 mM sodium fluoride, 10 μg/ml aprotinin and 10 μg/ml leupeptin. 100 μg protein lysates were resolved on a 10% SDS-PAGE gel, and western blots performed as previously described (Wang et al, 2012). Densitometry was performed using Image J.

Context pre-exposure fear conditioning

Mice were individually placed in the conditioning chamber for 10 min. No shocks were delivered in this phase of the experiment. Twenty-four hours later, all mice were placed in the conditioning context and, 5 s later, received a footshock (2 s, 1.0 mA). Twenty-four hours after immediate shock training, mice were placed in the conditioning context and freezing was assessed for a 2-min period. During this period, no shock was presented. For rolipram experiment, male mice received either vehicle (saline containing 2% DMSO, i.p. daily) or rolipram (1.25 mg/kg, i.p; in saline containing 2% DMSO, daily) treatment for 21 days followed by the 3-day paradigm of context pre-exposure fear memory test.

Morris Water Maze Task

6 months old mice (WT and *Cbp*S436A-KI, n=10-12/group) were trained on the hidden platform version of the water maze using a circular pool (122 cm diameter,83.5 cm depth, 22ºC) filled with 74.2 cm of water and made opaque with nontoxic white paint. The escape platform (10 cm diameter) was submerged 0.5 cm below the water surface. All testing was conducted under with 120lux lighting and an extra maze visual cue with "X" printed in black ink (2.9 cm thickness) on a white paper (13.5x15cm) was located on one wall. Acquisition was measured as latency to reach the platform and four possible start locations were pseudorandomly assigned to each trial. Each animal was given three 60 s trials to find the platform with a 15 s inter-trial interval across 7 days. A probe trial was then completed at day 8 and days 19 after the 7-day training, leaving the mice swim in the pool for 60 sec when the platform was removed. Ethovision tracking software was used to record behavior of the mice during testing and a full-automatic algorithm software developed by Steffany Bennett laboratory (Granger, et al., 2016) was used to determine search strategies during the training sessions.

Open field test

Mice were individually placed in a 45cm x 45cm x 45cm open field chamber for 10 min, and Ethovision software was used to record and analyze the distance traveled, locomotion speed, and amount of time the mice spent in respective zones (outer, middle, and center) of the box.

Antibodies

For immunohistochemistry, the primary antibodies used were rabbit anti-cleaved caspase 3 (1:1000; Cat#9661, Cell Signaling Technology, Beverly, MA), mouse anti-KI67 (1:200; Cat#556003, BD Pharmingen, Heidelberg, Germany), goat anti-doublecortin (1:200; Cat#sc-8066, Santa-Cruz Biotechnology), rat anti-BrdU (1:200; Cat#OBT0030G, Accurate Chemical), mouse anti-NEUN (1:500; Cat#MAB377, Chemicon), mouse anti-SOX2 (1:200; Cat#4900, Cell Signaling Technologies) rabbit anti-TBR2 (1:300; Cat#ab23345, Abcam), rabbit anti-GFAP (1:1000; Cat#ab7260, Abcam) and rabbit anti-p-CREB (S133)(1:100; Cat#9198, Cell Signaling). The secondary antibodies used were Alexa Fluor 555-conjugated goat anti-mouse IgG (1:1000; Cat#A21422, Molecular Probes), Alexa Fluor 488-conjugated goat anti-rat IgG (1:1000; Cat#A21208, Molecular Probe), Alexa Fluor 488-conjugated goat anti-rabbit IgG (1:1000; Cat#4412, Cell Signaling), Alexa Fluor 555-conjugated donkey anti-goat IgG (1:1000; Cat#A21432, Molecular Probes), Alexa Fluor 647-conjugated goat anti-mouse IgG (1:1000; Cat#A21237, Molecular Probes). For western blots, the primary antibodies were rabbit anti-p-aPKCζ/ι (T410/403)(1:500, Cat#9378, Cell Signaling), mouse anti- aPKCζ/ι (1:500; Cat#610175, BD), rabbit anti-p-CREB (S133)(1:500; Cat#9198, Cell Signaling), mouse anti-CREB (1:500; Cat#9104, Cell Signaling), rabbit anti-CBP (1:100; Cat#sc-583, Santa-Cruz).

Secondary antibodies for western blots were HRP-conjugated goat anti-mouse or anti-rabbit (1:4000; Cat#7076 and #7074, Boehringer Mannheim).

References

Carlo, C. N., and Stevens, C. F. (2011). Analysis of differential shrinkage in frozen brain sections and its implications for the use of guard zones in stereology. J. Comp. Neurol. 519: 2803–2810.

Eisch A.J., Barrot M., Schad, C.A., Self, D.W. and Nestler E.J. (2000) Opiates inhibit neurogenesis in the adult rat hippocampus. Proc Natl Acad Sci U. S. A. *97*, 7579-7584.

Gardella, D., Hatton, W. J., Rind, H. B., Rosen, G. D., and von Bartheld, C. S. (2003). Differential tissue shrinkage and compression in the z-axis: implications for optical dissector counting in vibratome-, plastic- and cryosections. J. Neurosci. Methods 124: 45–59.

Gould, E., Beylin, A., Tanapat, P., Reeves, A., Shors, T.J. (1999) Learning enhances adult neurogenesis in the hippocampal formation. Nat. Neuroscience *2*, 260-265.

Granger, M.W., Franko, B., Taylor, M.W. Messier, C., St George-Hyslop, P. and Bennett, S.A. (2016) A TgCRND8 Mouse Model of Alzheimer's Disease Exhibits Sexual Dimorphisms in Behavioral Indices of Cognitive Reserve, J.Alzheimers Dis. Feb 10 [Epub ahead of print].

Guillery, R.W. and Herrup, K. (1997) Quantification without pontification: choosing a method for counting objects in sectioned tissues. J Comp Neurol *386*, 2-7.

Jayatissa, M.N., Henningsen, K., West, M.J. and Wiborg, O. (2009) Decreased cell proliferation in the dentate gyrus does not associate with development of anhedonic-like symptoms in rats. Brain Res *1290*, 133-141.

Malberg, J.E., Eisch, A.J., Nestler, E.J. and Duman, R.S. (2000) Chronic antidepressant treatment increases neurogenesis in adult rat hippocampus. J Neurosci. 20, 9104-9110.

Mouton, P. (2002) Principles and Practices of Unbiased Stereology: An Introduction for Bioscientists (The Johns Hopkins University Press, Baltimore).

Miller, D.J., Balaram, P., Young, N.A. and Kaas, J.H. (2014) Three counting methods agree on cell and neuron number in chimpanzee primary visual cortex. Front. Neuroanat. 8:36.

Olariu, A., Cleaver, K.M. and Cameron, H.A. (2007) Decreased neurogenesis in aged rats results from loss of granule cell precursors without lengthening of the cell cycle. J Comp Neurol *501*, 659-667.

Pakkenberg, B. and Gundersen, H.J. (1988) Total number of neurons and glial cells in human brain nuclei estimated by the disector and the fractionator. J Microsc *150*, 1-20.

Wang, J., Gallagher, D., DeVito, L., Cancino, I., Tsui, D., He, L., Keller, G.M., Frankland, P.W., Kaplan, D.R. and Miller, F.D. (2012) Metformin activates atypical PKC-CBP pathway to promote neurogenesis and enhance spatial memory formation. Cell Stem Cell, *11*, 23-35.

West, M.J. and Gundersen, H.J. (1990) Unbiased stereological estimation of the number of neurons in the human hippocampus. J Comp Neurol *296*:1-22.

West, M.J., Slomianka, L. and Gundersen, H.J. (1991) Unbiased stereological estimation of the total number of neurons in thesubdivisions of the rat hippocampus using the optical fractionator. Anat. Rec. *231*, 482-497

Wojtowicz, J.M., and Kee, N. (2006). BrdU assay for neurogenesis in rodents. Nat. Protoc. 1, 1399–1405.